University College of Southeast Norway

www.usn.no

FMH606 Master's Thesis 2017
942 Energy and Environmental Technology

Experimental measurements of diesel spray in an inert gas generator

by

Lena Dyveke Weber

Faculty of Technology, Natural sciences and Maritime Sciences
Campus Porsgrunn

University College of Southeast Norway

www.usn.no

Course: FMH606 Master's Thesis, 2017

Title: Experimental measurements of diesel spray in an inert gas generator

Number of pages: 50

Keywords: Atomization, spray, LNG, diesel pilot flame, shadowgraph technique, high-speed camera, image processing, droplet distribution measurements

Student: Lena Dyveke Weber

Supervisor: Joachim Lundberg

External partner: Odd Ivar Lindløv

Availability: Open

Approved for archiving: _____

(supervisor signature)

A 90° Y-jet atomizing nozzle with 3 bores was experimentally tested in a science facility at University College of Southeast Norway. The nozzle is producing a diesel fuel spray for a pilot flame in an IGG system for marine shipping of LNG. The diesel fuel was replaced by water for environmental reasons in the experiment.
The spray was photographed with a high-speed camera using an IR laser for a light source and the images were processed using a user defined method for droplet diameter determination. The measured droplet diameter distribution and the calculated SMD indicates large droplets at elevated pressures and the nozzle produces a large span of droplets. The nozzle was performing adequately within the turndown ratio, with the precaution that the span of droplet diameters is within reason for the users of the nozzle. The span of the droplet sizes increased with pressure increase.
Findings of non-spherical droplets, bulges and sheets of water were unavailable for measurement due to limitations of the image processing technique, suggestions for further analysis are presented.
Replacing water for diesel was an acceptable method and is recommended for similar non-combusting experiments. However, further research of the coherence between water and diesel spray is recommended.

Preface

This master thesis has been developed during the spring semester of 2017, as a final requirement of the graduate master program 942 Energy and Environmental Technology at University College of Southeast Norway. The master thesis task was kindly provided by Wärtsilä Moss AS via their contact Odd Ivar Lindløv. See Appendix A Task Description.

Software used in this report was Photron FASTCAM Viewer, Microsoft Office (Excel and Word) and MATLAB. The reader of this report should be equipped with a general understanding of fluid dynamics, image processing techniques and combustion processes.

Sadly, I was delayed due to equipment failure in this thesis. The intended laser for the experiment, the Copper Vapor Laser (CVL), failed twice. A change of laser equipment was necessary. The Firefly, an IR laser was implemented in the rig, which was time consuming. Because of the delay only the 90° nozzle was tested, unfortunately the 55° was not tested. Due to the double failure, the experimental results were analyzed later than scheduled, forcing me to apply for an extension of the hand in. My application was kindly granted by Dean, Morten C. Melaaen, and I got two more weeks for analysis and writing my report. Although with the two weeks extension, the quality of this report is affected by this shortness of time. I sincerely hope there is something viable in this report non-the-less.
The final and successful experiment was conducted in approximately twelve hours, however, with the work of the setup of equipment, calibration process and waiting for other students to finish their lab work, the time consumption was approximately additional ten days. For image processing the intent was to use a similar method to Associate Professor, Joachim Lundberg, doctoral dissertation. However, due to the change in the light source (IR laser) the data was not viable for that method.

A literature review was also an intention to perform in this report, due to delays the literature presented in this report is directly linked to the experiment and the method for image processing.

The greatest of gratitude and appreciation goes to my supervisor, Joachim Lundberg, this semester has been a roller-coaster ride between equipment failure and hope for success. If not for Joachim, I'm not sure how it would have ended. Also, gratitude is directed to Odd Ivar Lindløv and his colleagues from Wärtsilä Moss AS for this great task, equipment and their engagement in following up the results of the experiments.

I want to express love and appreciation for my best buddy and partner for life Petter Næs Larsen, *"To infinity and beyond,"* I love you.

And finally, a big shout-out to my study group @B-1008, you know who you are, and you're freaking fantastic.

Porsgrunn, 29.05.17

Lena Dyveke Weber

Nomenclature

Abbreviations

BLEVE	Boiling Liquid Expanding Vapor Explosion
BOG	Boil Off Gas
GUI	Graphical User Interphases
IGG	Inert Gas Generation
IGG-GCU	Inert Gas Generation-Gas Combustion Unit
LNG	Liquid Natural Gas
SMD	Sauter Mean Diameter [µm]

Symbols

$\sum_{j=1}^{\infty}$	Summation of a set of data starting from 1 to infinity
D_{pq}	Mean diameter based on factors p and q
$n_j d_j^p$	Summation of all droplet sizes to the power of p
$n_j d_j^q$	Summation if all droplet sizes to the power of q
p	Mean diameter factor based on application area
q	Mean diameter factor based on application area

Contents

1 Introduction

Atomization is a method to break up bulk liquid into droplets, creating a spray. An example of natural occurring atomization is mist from sea water and waterfalls. Atomization of spray is used in many industries; the pharmacy industry produces aerosol medicine, such as asthma inhalators. In agriculture, coating of food with pesticides are important to preserve and keep the food fresh. Mainly, atomization is used in combustion processes such as transport vehicles (cars, trailers, ships and aircrafts) and for combustion in engines and boilers for industrial use, similar to the context of this report task description (Appendix A Task Description) for this thesis.
A spray can be defined as poly- or monodisperse, which means the droplets are of varying or equal sizes. From the information given to this thesis, it is known that the spray is polydisperse. However, it is unknown how much variation there is between the droplet sizes. It is of interest to investigate the diameter span in the spray and the distribution of droplet sizes.

1.1 Background

This thesis problem description, look to Appendix A Task Description, was provided by Wärtsilä Moss AS. Where a project group is developing a more efficient inert gas generation (IGG) system for liquid natural gas (LNG) carrying ships. The IGG system combusts the boil-off gas (BOG) from (LNG) with help from a pilot diesel flame. Look to Figure 1-1 for illustration of IGG system. The BOG is combusted continually and the energy released from the LNG can be utilized, potentially increasing transport efficiencies by cost savings and lowering the increasing demand of diesel fuel [1].

Figure 1-1 Inert gas generation system with a burner/scrubber unit for inert gas generation [2]

A seawater scrubber, part of the gas combustion unit (GCU), will clean the exhaust gases leaving clean exhaust. The inert gas produced in the IGG system is redirected to the LNG tanks to prevent air from entering the tank.

Evacuation of residual BOG from LNG to air frequently occurs, however, due to environmental hazards and the expanding regulation of maritime emission control, the use of this method is decreasing [3]. The BOG from carrying LNG needs to be further processed onboard ships, due to its high evaporation rate, it boils at approximately -162°C. The BOG can cause hazardous situations if not handled correctly, due to the risks occurring from an increase in pressure and the volatility of LNG when mixed with air. By managing the BOG properly, accidents caused by a can be avoided, such as fires and BLEVE's [1, 4].

The pilot flame is initiated when the LNG-to-inert gas mixture is too lean to combust, maintaining the combustion of the BOG. The IGG system, although with the help of a pilot flame, needs further investigation to be optimized. It is of interest to sufficiently combust the dual fuel (LNG and diesel) as well as maintaining a low emission of pollutant products, such as carbon monoxide (CO).

The flame profiles are difficult to determine due to many unknown factors in the combustion process. Look to Figure 1-2 for sketched suggestions of the flame profile based on three designs for the gas combustion unit (GCU). The different suggestion has been made for determination of the flame profile; the profiles were tested for design No.2 recently, unfortunately with unsuccessful results. Therefore design No. 1 is the next step for the project group at Wärtsilä Moss AS to achieve a sufficient combustion process.

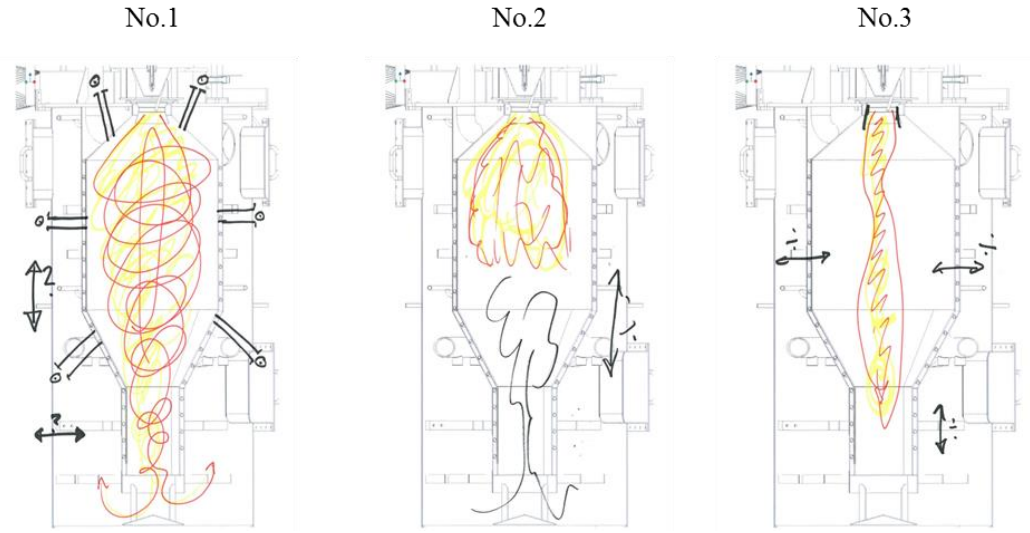

Figure 1-2 Suggestion of GCU designs [5]

When optimizing the IGG system, it is natural to investigate the diesel spray characteristics due to the instability of the flame profile. Wärtsilä Moss AS uses a Y-jet nozzle, with a turndown ratio of 1:10, look to Figure 1-3 for a picture of the atomizer nozzle. Information about the spray characteristics is not provided by the manufacturer of the nozzle, drawing out questions about the spray characteristics being a contributor to difficulties combusting the fuel properly.

Figure 1-3 Atomizer 24-Y-90°-00-3 from Fluidics Instruments, look to Appendix F Nozzle 24-Y for technical information.

1.1.1 LNG in the global marked

The use of (LNG) in marine technology and other areas are expanding [6]. LNG is used for energy production onshore, and it is usually transported in carriers on ships. The LNG is more and more frequently utilized for propulsion in marine shipping, where the fuel is utilized in dual fuel engines [7]. The LNG consists of mainly methane (CH_4), which is classified as a global warming gas. Several sources state that LNG/methane has 84 times more global warming potential (GPW) than CO_2 for a 100 year period and others are claiming 28-34 times more potential than CO_2 for a period of 20 years [8, 9]. Emitting more than a minimum should be can be avoided with correct handling and following regulations [10]. However, LNG is an attractive fuel due to its low emission e.g. CO_2, SO_2 and NO_x and its potential in the global market continue to grow [8].

1.2 Objective

The aim is to measure the diesel spray characteristics from the Y-jet nozzle via a non-combusting experiment. However, due to environmental concerns, the diesel is replaced by service water, assuming that the water droplets is similar as diesel droplets. The droplets diameters will be measured with the use of shadowgraph technique, high-speed video and image processing technique for analysis, according to Associate Professor Joachim Lundberg's doctoral dissertation thesis "Image-based sizing techniques for fire water droplets" [11].

1.3 Report structure

In this report, there are seven chapters in total. It is advised to read the report chronologically. Chapter 2 provides theoretical information about Atomization of spray. Chapter 3 presents the methods of image processing and analysis tools used in the report. Chapter 4 describes the procedure for the experiment and the equipment used. The results of the experiment are presented in Chapter 5. Chapter 6 debates the results and theoretical information presented in this thesis. Chapter 7 completes the report with a conclusion. The coherent appendices and references can be read at the time the reader has the need for additional information or as referred to in the text.

2 Atomization of spray

The breakup of a liquid jet can be achieved by several methods, in this thesis the liquid is pressurized, creating oscillations and perturbations from cohesive forces inside the system. Air, kept at a constant pressure level, assists the disintegration of the liquid jet. The atomizing nozzle used in this report is a Y-jet atomizer with three bores uniformly placed, with respect to the nozzles vertical axis. In "Atomization of spray" by Lefebvre in 1989, it is described that a Y-jet nozzle creates a conical hollow spray due to the rapid merging of the individual sprays, depending on the angle of each spray and the number of sprays [12]. In this thesis, the sprays are narrow and do not form a conical spray. Instead, three individual sprays occur.

The disintegrations of jets are often divided into two stages; Primary atomization and secondary atomization. Primary atomization occurs when the jet is about to exit the nozzle, at the point where the two fluids intersect. Secondary atomization occurs on the outside of the nozzle. The aerodynamic forces exceed the internal forces (e.g. surface tension and viscosity) of the droplet resulting in further breakup. The droplets will keep disintegrating until equilibrium between external aerodynamic forces and internal forces is achieved. Lefebvre refers these force relations, in the secondary atomization, as critical size, which means that if a droplet is larger than the critical size, it will continue disintegrating. Note that if the aerodynamic forces decrease during the breakup time, further breakup of the droplet may not occur although the disruptive forces affecting the liquid is still present [12].

Hinze identified and categorized deformation types of droplets in 1955, where the categories were as follows; lenticular droplets (spheroid shape), elongated formed droplets (cigar shape) and bulgy droplets, see Figure 2-2. The shapes could be a result of aerodynamic forces such as dynamic pressures and stresses impacting the droplets. Surrounding aerodynamic forces are pulling and dragging the droplets apart. However, as mentioned from Lefebvre, the droplets do not necessary breakup further. Drag forces inflicting the droplet from the surroundings can impact the droplets shapes and drag is likely the reason for non-spherical droplets, like when you blow on a droplet of water. Lefebvre also mentions a disintegration of droplets in still air, look to Figure 2-1, where the droplets disintegrate by surrounding forces [12, 13].

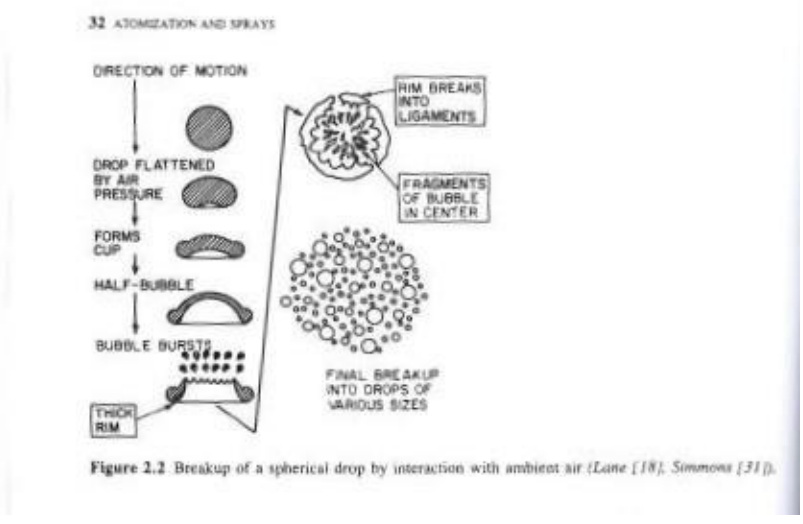

Figure 2-1 Disintegration of droplets in still air [12]

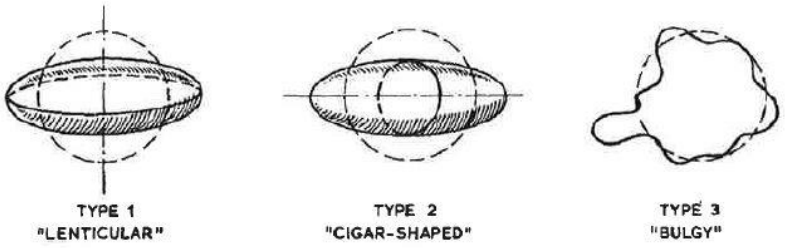

Fig. 1. Basic types of globule deformation.

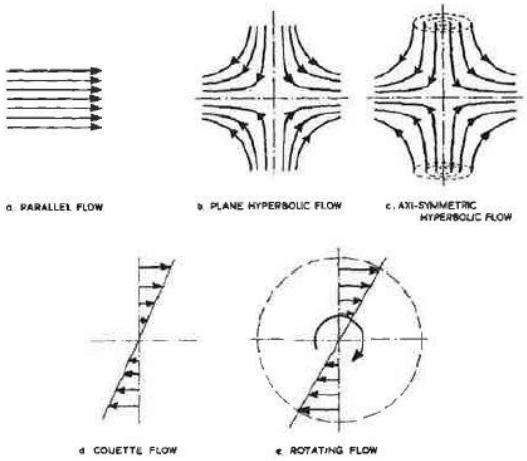

Fig. 2. Flow patterns that can cause one of the basic types of globule deformation.

TABLE 1.—POSSIBLE CONDITIONS FOR BREAKUP OF A GLOBULE

Type of deformation	A. Dynamic pressures			B. Viscous stresses		
	Flow pattern around the globule					
1. Lenticular ..	(*a*) Parallel	(*c*) Axisymm. hyperbol.	(*e*) Rotat.	(*a*) Parallel	(*c*) Axisymm. hyperbol.	(*e*) Rotat.
2. Cigar-shaped	(*b*) Plane hyperbol.	(*d*) Couette		(*b*) Plane hyperbol.	(*d*) Couette	
3. Bulgy	(*f*) Irregular					

Figure 2-2 Categories for droplet deformation types based on surrounding flow patterns [13]

Many small droplets in a fuel spray create a higher surface area and the volume per droplet is low, resulting in a quick combustion reaction and a fast heat release. Many large droplets also create a large surface area. However, the volume per droplet is greater and could result in a slow reaction. Larger droplets can be more difficult to completely combust as the droplet evaporates slower, which could result in incomplete combustion. The larger droplets evaporation time could exceed the space in the combustion chamber and stick to walls or other obstacles, possibly creating a pool of unburnt fuel and smoke. Therefore, the stability of a flame profile can be determined by the distribution of droplets in a fuel spray [12, 13].

3 Image processing

This chapter describes the method of measuring droplets with the use of computational tools MATLAB and Microsoft Excel as well as Photron FASTCAM Viewer. The chapter also describes the method of computing the Sauter Mean Diameter.

Shadowgraph technique is applied in many fields of atomization of spray. E.g. a light source is projected onto the object/field of interest, creating a shadow outline of the object(s) silhouette. In this thesis, the droplets in a spray are the object of interest, and a light source is scattering light at the spray creating shadows that outline the droplets in the spray, making them visible for measurement and analysis. The main source of error is the fact that the measured object is a shadow and not object itself, which is the main drawback of the shadowgraph technique [14, 15].

The intended image processing technique in this thesis was to use a similar method that Lundberg developed in his doctoral dissertation. The program was designed to measure droplet sizes and velocities by managing the image processing on three parallel images at the same time. Meaning the program brings a consolidated impression of how the properties in a sprays changes over time. The shapes of the spray is not a limiting factor in Lundberg's program [11].

3.1 Droplet distribution measurement

Measuring the distribution of droplets can be achieved with the use of two methods according to the book "Combustion Engineering," by Borman and Ragland. The first mentioned method is spatial sampling technique (instantaneously) and the second method is temporal sampling (over time). Spatial sampling of the distribution is e.g. achieved with high-speed photography with light scattering at the spray and is further analyzed with the help of image process techniques, similar to this thesis. The temporal sampling technique is also known as the flux method registers the number of droplets through an area of a surface like a "*tollgate*,". The measurements from temporal can also be conducted through photography or other digital measurement techniques [16].
Pfeifer et al. used both spatial and temporal measurements in their paper on droplet size and velocity distribution to be able to measure non-spherical droplets [17].

3.2 Calibration of Pixel Size

Determination of pixel size was performed with a reticle globe, type Patterson Globe, look to Figure 3-1 for a picture of the globe and Table 4-1 for more information about the Patterson Globe. The calibration of pixel size was conducted without spray present.

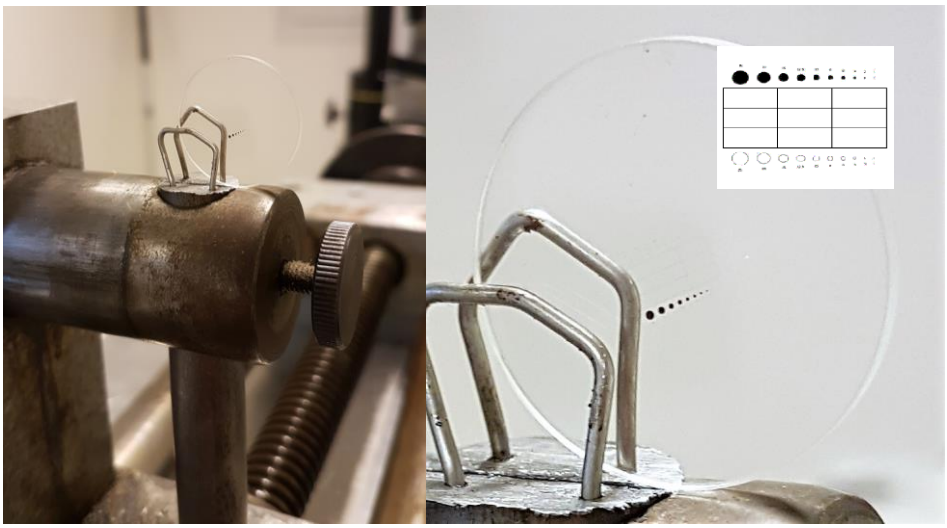

Figure 3-1 Patterson Globe mounted on a translation screw

The depth of field of the camera was set on the globe, which was placed perpendicular to the field of view, 60 cm from the camera lens to the globe. The largest circle on the globe has a reference size of 450 µm. In Photron FASTCAM Viewer, with respect to the size of the largest circle, one pixel was measured to be approximately 8 µm. Look to Figure 3-2 for a picture of the calibration process. The size of one frame was measured to be approximately 0.822 cm.

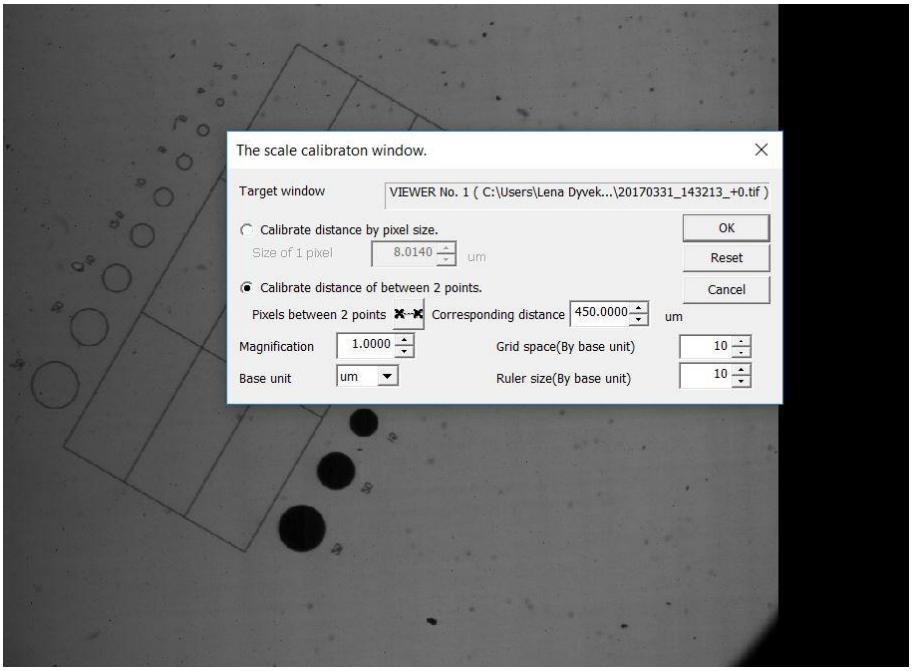

Figure 3-2 Calibration of pixel size in Photron FASTCAM Viewer

3.3 Droplet diameter measurement and analysis

3.3.1 Droplet diameter determination in MATLAB

To be able to determine the droplet sizes, an image processing script in MATLAB were developed in collaboration with Associate Professor, Joachim Lundberg, at the University College of Southeast Norway. The image processing technique in MATLAB can be described as a user defined method for droplet diameter determination, see Appendix B MATLAB Script for the entire code.

The frames were imported from a selected library, and the chosen frames were illustrated in a separate window, a set of frames was chosen for each measurement sequence. The code creates a manual operator, which means the measurements were performed with a computer mouse. The operation was to find the x, y coordinates outlining the droplet in the frame. The x, y coordinates were used to calculate the diameter via a circular help size. The code returned the diameter sizes in a matrix. The number of diameters allowed to measure (m_d) in one frame was set depending on how many droplets there were to measure. This setting was determined before the code ran, it was, therefore, a good method to use the Photron FASCAM Viewer to look through the videos prior to the measurements. Look to Figure 3-3 for an image of the user defined droplet diameter determination operator.

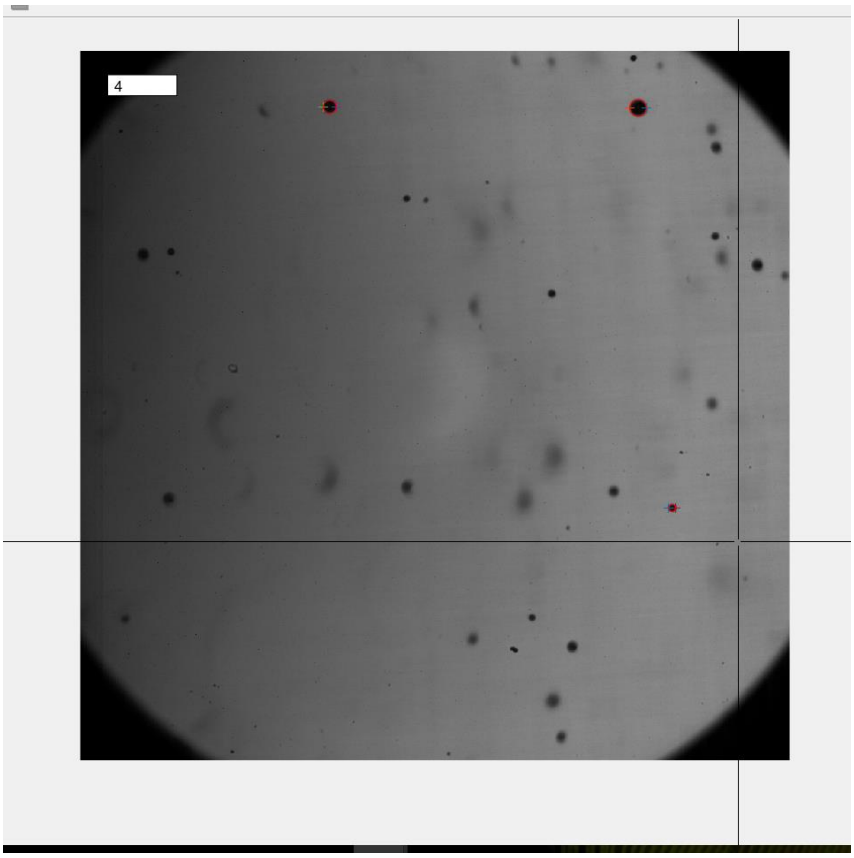

Figure 3-3 Image from diameter measurements in MATLAB

Approximately 100-200 droplets were measured in MATLAB for each video, giving an approximation of 2250 measured droplets, among millions of droplets recorded in total. As Lundberg states in his doctoral dissertation from 2015, the number of measurements should reflect the depth of the analysis. In this thesis, the time aspect and the limitation regarding the user defined method for droplet determination does not allow hundreds of videos to be examined [11].

3.3.2 Droplet diameters in Microsoft Excel

The droplet diameters measured in MATLAB was further processed in Microsoft Excel, where the data was sorted, and graphical illustrations were produced with the help of built-in tools.

3.4 Sauter Mean Diameter (SMD)

Droplet mean diameters were standardized by Mugele and Evans in 1951 [18], which has been referenced by several researchers such as Lefebvre [12]. The field of application is the determining factor for which mean diameter to use, the most common mean diameter for heat and mass transfer is the Sauter Mean Diameter, also referred to D_{32}. It is a numerical description of the liquids ability to evaporate, due to its relation to the droplets volume to surface ratio, that is representative for the whole spray.

Equation 3.1 describes the calculation of the standardized mean diameters from Mugele and Evans

$$D_{pq} = \left[\frac{\sum_{j=1}^{\infty} n_j d_j^p}{\sum_{j=1}^{\infty} n_j d_j^q}\right]^{1/p-q} \tag{3.1}$$

Where $p = 3$
$q = 2$
d= measured diameter for calculation the SMD

According to Lefebvre, a mean diameter alone cannot describe a spray. However, it can be used as a tool for determining a part of the spray characteristics. A spray with high SMD values indicates that the volume to surface ratio of the dispersed liquid is high, and the rate of evaporation is affected by that. The SMD is, simply speaking, a parameter which can contribute to determining the mass and heat transfer properties for a fuel spray [12].

4 Experiment and Equipment

This chapter describes the experimental setup, procedure and equipment. High-speed videos of the spray were made, in total 46 videos, where 15 of the videos was further analyzed. For a listing of equipment look to Table 4-1. The experimental setup is similar to Lundberg's experimental rig. However with other process equipment [11].

Water was replacing diesel in the experiment, a necessary precaution considering the safety of people and the surroundings. Diesel dissipates dangerous fumes and it is easily ignited and can contaminate equipment and cause fires. The main difference between atomization of water vs. diesel oil is presumed to be that the water droplets are larger than diesel droplets, mainly due to water having a higher surface tension and density. A study from Sulaiman et al. comparing the droplet sizes of water and diesel concurred with the assumption that the water droplets are slightly larger and show approximately the same trends compared with diesel. Their conclusion was that water could be a good replacement for diesel in non-combusting experiments where diesel is not suitable to use [19].
For additional safety precautions regarding the experiment, look to Appendix C Safe Job Analysis (SJA).

4.1 Experimental setup and procedure

The experimental rig was located in a science facility at University College of Southeast Norway. Look to Figure 4-1 for a simplified illustration of the experimental setup.

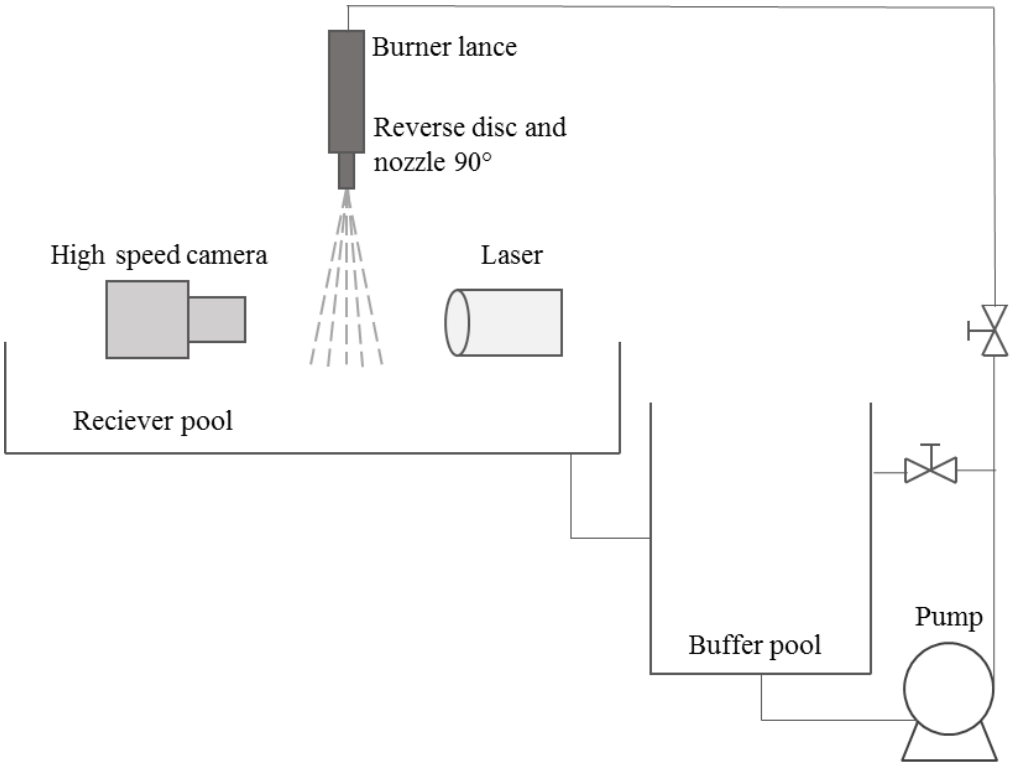

Figure 4-1 Illustration of experimental setup

The rig consisted of a large container (caravan) to protect the outside environment from laser beams. The container was also meant as an equipment protector, shielding the equipment from outside activity and collecting spilled water. Look to Figure 4-2 for a picture of the container.

Figure 4-2 Container

Equipment placed inside the container was a high-speed camera with a long-distance microscope lens and an IR laser, see Figure 4-3.

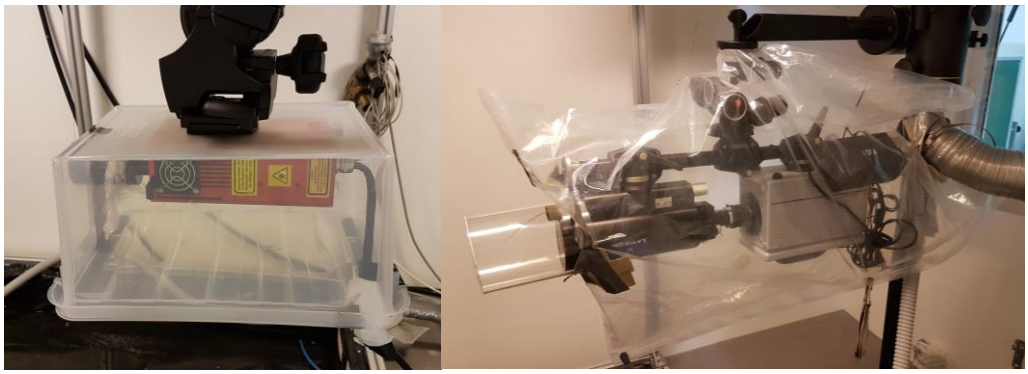

Figure 4-3 Picture of the IR laser (to the left) and high-speed camera with long-distance microscope (to the right)

Furthermore, inside the container, a burner lance with two pressure gauges was mounted on a traverse and auxiliary equipment such as protective tubes for wires and transmitting optics. See Figure 4-4 for pictures of the burner lance, high-speed camera, laser and spray.

Figure 4-4 Picture of the burner lance, high-speed camera and laser. Picture to the right shows the sprays at initial pressure

The laser was connected to the camera for synchronization, look to Appendix D Experimental procedure for settings of camera and laser. The camera had transmitting optics connected to a laptop for visual monitoring and recording. The software used for recording was Photron FASTCAM Viewer.

Outside of the caravan, a gear pump delivered water to the system. Compressed service air from the facilities compressor system delivered the atomizing air. The mass flow of water and air was measured via two Coriolis meters and logged manually. Look to Figure 4-5 and Figure 4-6 for pictures of the mass flow equipment.

Figure 4-5 Frequency controller, gear pump, and a Coriolis meter for mass flow measurement of water

Figure 4-6 Regulator for air supply and Coriolis meter for air mass flow measurement

The buffer pool was filled with water before the experiment and the receiver pool guided the accumulated water back to the buffer pool. The buffer pool was emptied after use, look to Figure 4-7 for a picture of the buffer pool.

Figure 4-7 Buffer pool

The nozzle was positioned at an angle of 45°, perpendicular to the camera and laser plane. The center of the spray was measured 60 cm from the camera lens and as mentioned in Chapter 3, depth of field was set at that point. The nozzle delivered three separate conical sprays, where one spray was investigated due to simplicity. Atomizing air was fixed at 6 barg, therefore, regulation of the spray was via the liquid mass flow and pressure. For sufficient investigation of the spray, it was determined to measure several positions in the spray width. The positions were determined via extrapolation, from a plane perpendicular to the spray center. Each step in the perpendicular plane was 5 cm and the path of the spray determined the measuring points along the x-axis. Look to Figure 4-8 for an illustration of the positions. High-speed video of all tests in the experiment was performed.

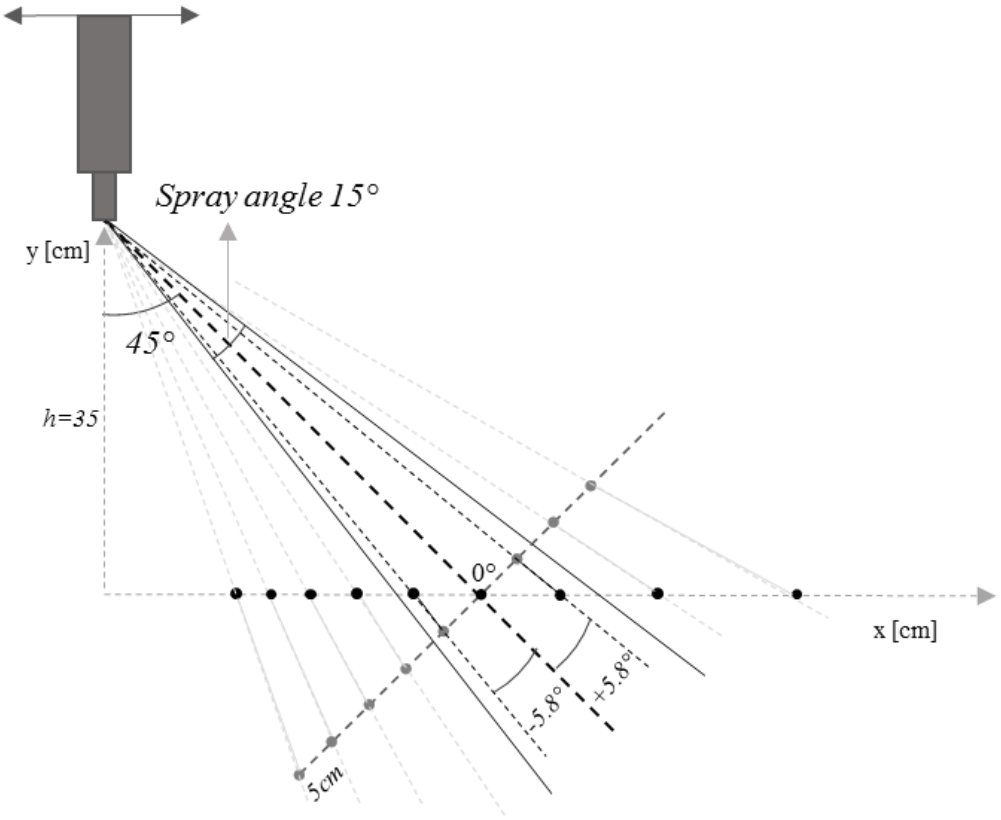

Figure 4-8 Measurement points for high-speed video with respect to the center of spray.

In addition to the measuring of several points along the x-axis, different pressures of water were tested. Tests of positions and pressure was performed and video was taken at initial conditions 1 barg, according to project description [20]. Furthermore, videos of the spray was performed at pressure 3 barg, 5 barg, 7 barg and 9 barg. The pressure stages were tested at each measuring point along the x-axis. This resulted in 46 videos of the spray (video of the highest pressure test in the center of spray was conducted twice due to uncertainties is the system parameters).

The turndown ratio according to Figure 4-9, with the initial condition as a starting point, the minimum mass flow would be around 12.5 kg/h. The maximum, based on turndown ratio of 1:10, would be approximately 125 kg/h, which would give a maximum test pressure of 6.3 barg. However, Figure 4-9 is based on fine diesel oil which has lower density than water [21]. Furthermore, the water mass flows were not known before the experiment, therefore, test pressures 1, 3, 5, 7 and 9 barg was selected to ensure sufficient coverage of mass flows for testing. The surroundings of the spray were ambient room tempered air.

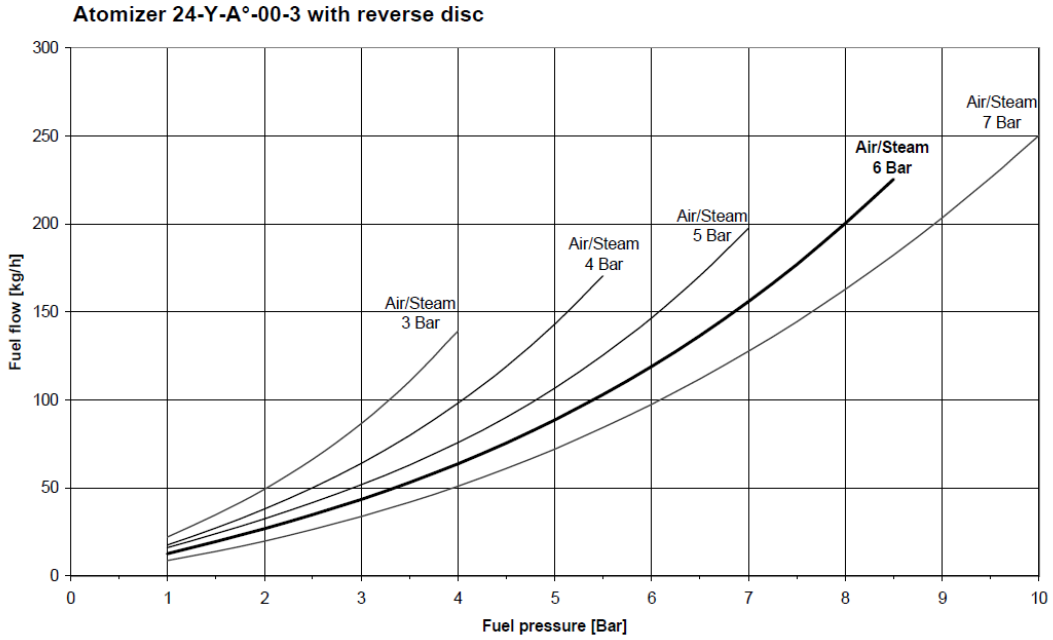

Figure 4-9 Pressure curves with mass flow based on diesel, provided from Wärtsilä Moss AS [20]

4.1.1 Equipment

Table 4-1 shows a listing of equipment used in the experiment.

Table 4-1 Equipment

Equipment	**Name/ Identification**	**Properties/Description**	**More information**
Gear pump	Selvsugende tannhjulspumpe	Deliver water to burner lance	Appendix H Gear Pump
Regulator	Reg 300 0-12 barg	Regulation of the compressed air (fixed at 6 barg)	No additional information available
Frequency controller	MOVITRAC® MC07B0008-2B1-4-00	Control the mass flow of water	http://www.seweurodrive.com/produkt/movitrac-mc07b.htm
Coriolis mass flow meter	Yokogawa ROTAMASS 3 Series Coriolis Mass Flow and Density Meter	Mass flow measurements for air	https://www.yokogawa.com/fld/pdf/rota/IM01R04B04-00E-E.pdf
Coriolis mass flow meter	Endress+Hauser Proline Promass 83F	Mass flow measurements for water	https://portal.endress.com/wa001/dla/5000275/1921/000/02/TI00101DEN_1314.pdf
Burner lance	FI 24-HA-SA-E	Deliver water and air through the nozzle	Appendix G Burner lance 24
Y-jet nozzle 90° and reverse disc	Fluidics Instruments B.V. Atomizer 24-Y-90°-00-3 FI Reverse disc 24-R	Nozzle delivers three conical sprays. Reverse disk changes the position of liquid and air, streaming on the outer side of nozzle and atomization air in the inner part of the nozzle.	Appendix E Nozzle with reverse disc Appendix F Nozzle 24-Y
Gauges	AB Pressure Gauges	Accuracy standard EN 837-1 Class 1.6	No additional information available
High-speed camera	ultima APX-RS, monochrome model	High-speed camera with grayscale color	https://photron.com/wp-content/uploads/2014/04/ultima_APX-RS.pdf

Long-distance microscope with zoom lens	Questar QM-1 by LaVision and a 172mm 0.9X Positive Lens (standard accessory)	Focal length from 56cm to 152cm	http://www.company7.com/questar/microscope/qm1.html [22]
Patterson Globe		Reticle for calibration of pixel size	https://www.microscopeworld.com/t-patterson_globe_microscope_reticle.aspx
Laser and diffuser	Firefly High-Speed Imaging Laser IR 808 nm Oxford Lasers. 5cm diffuser	Light beams create shadows making the droplets visible (shadowgraph technique)	https://www.oxfordlasers.com/imaging/imaging-product/firefly-piv-and-imaging-laser/
Photron	PFV Photron FASTCAM Viewer	Image viewer, recorder and editor for high-speed video	https://photron.com/high-speed/cameras/pfv-photron-fastcam-viewer/
Water for spray	Service water from facility	A replacement for diesel oil. Approximately 5°C	No additional information available

5 Results

Results of experiments and analysis in MATLAB, Excel and Photron FASTAM Viewer are presented in this chapter.

5.1 Drop size distribution

5.1.1 SMD

Table 5-1 shows the calculated SMD for all pressure tests based on the measured diameters. The SMD for the center of spray are the largest, the SMD +5.8° from the center of the spray is second largest (except for pressure test 5 and 7 barg) and -5.8° from the center of the spray is the smallest (except for pressure test 5 and 7 barg) when comparing all three.

Table 5-1 SMD calculated in Excel

Pressure, water [barg]	**SMD [µm]**		
	-5.8°	**0°**	**+5.8°**
1	93	103	106
3	92	118	104
5	130	146	117
7	138	155	130
9	298	325	300

Figure 5-1 shows the SMD increases as the water pressure increases. The SMD has the highest increase from pressure 7 to 9 barg. The span of the SMD is from approximately 90 to 325 µm.

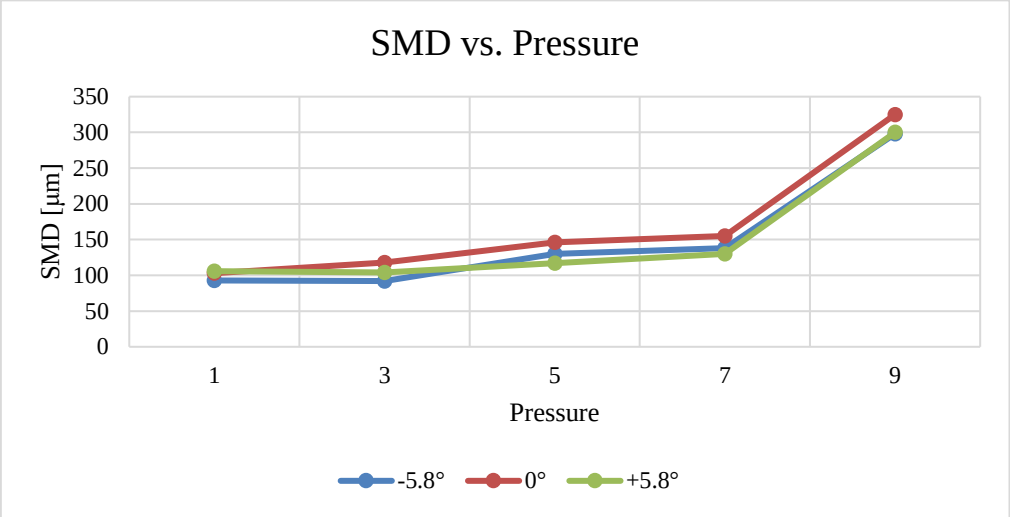

Figure 5-1 SMD vs. pressure

5.1.2 Occurrence

Figure 5-2 shows that the highest occurring sizes are 70-79 µm for the center of the spray (0°). In +5.8° from the center the highest occurring sizes are 80-89 µm and that the highest occurrence of sizes is in the range of 70-89 µm for the position -5.8° from the center. Figure 5-2 also shows that the distribution pattern follows approximately the same trend for each position from the center. The span of the droplets in this test are from approximately 15 to 200 µm, with the highest occurring sizes in 70-89 µm.

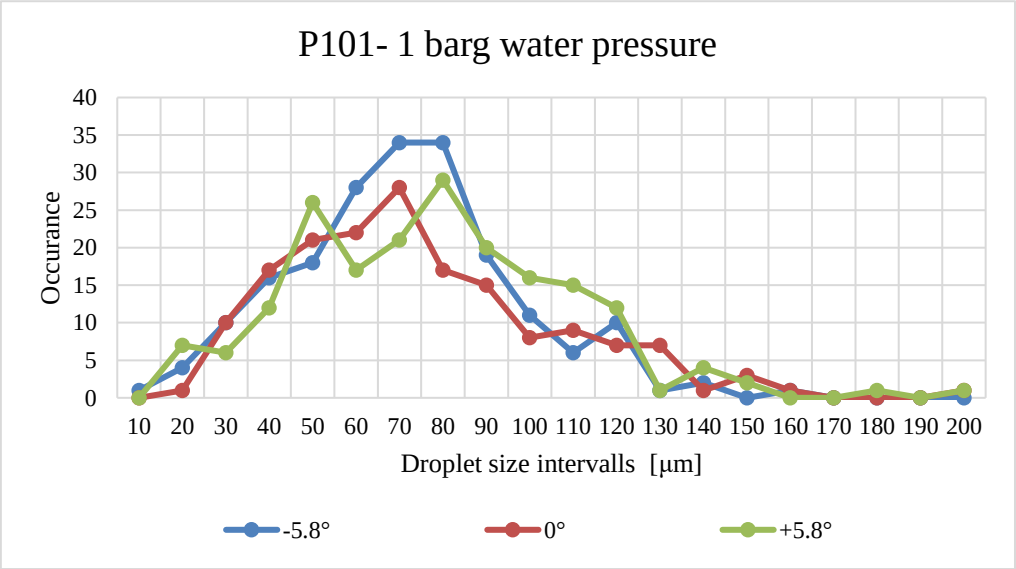

Figure 5-2 Size distribution by occurrence, liquid pressure 1 barg

Figure 5-3 shows the highest occurrent size interval are the same for all three positions, 60-74 µm. Figure 5-3 also shows that the distribution pattern follows approximately the same trend for each position from the center. The span of the droplets in this test are from approximately 10 to 245 µm.

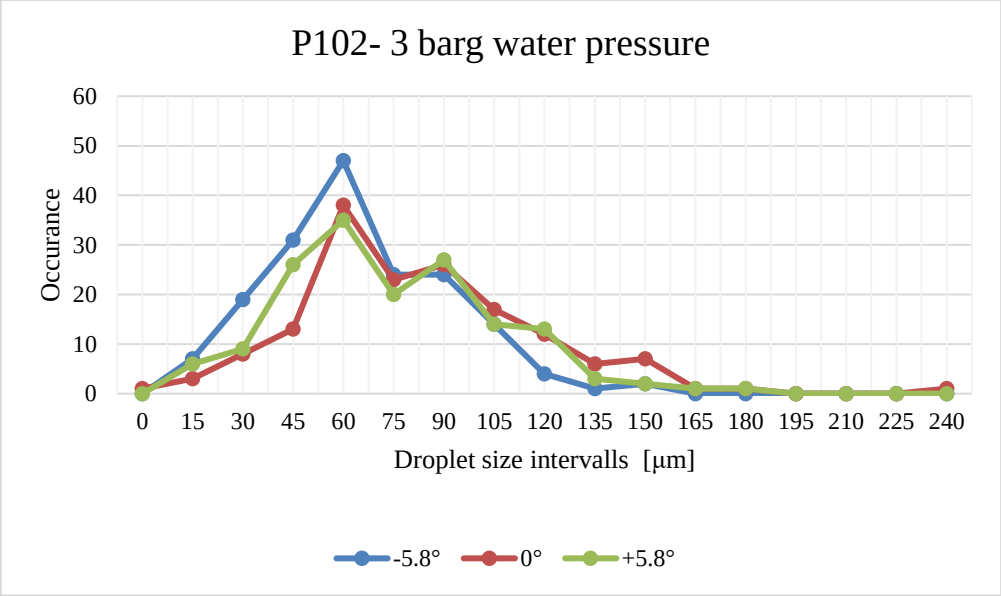

Figure 5-3 Size distribution by occurrence, liquid pressure 3 barg

Figure 5-4 shows that the highest occurring sizes are 70-84 µm for all three positions. The figure also displays a high occurrence in interval 100-114 µm for in the center of spray and +5.8° the right from center. Figure 5-4 also shows that the distribution pattern almost similar and they all peak in the same position (70-84 µm). The span of the droplets in this test are from approximately 20 to 260 µm.

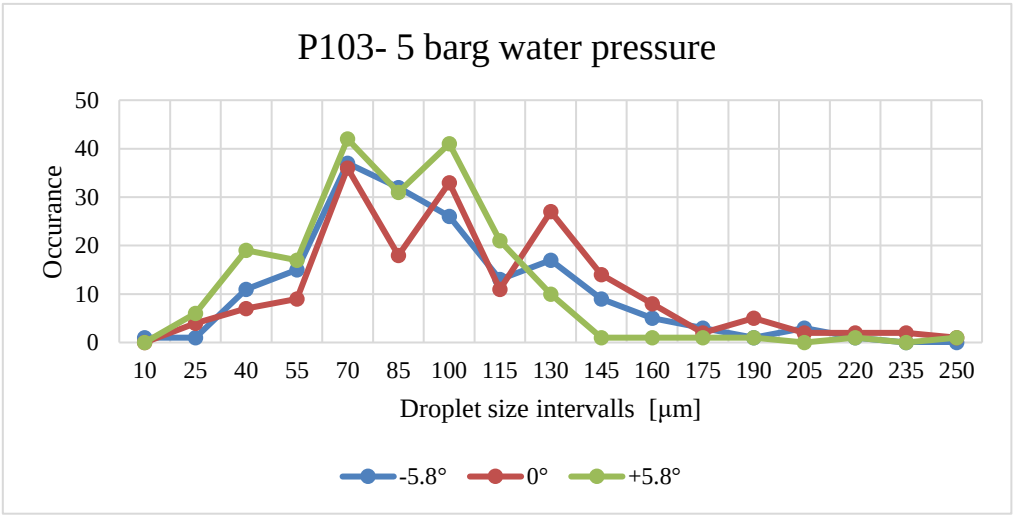

Figure 5-4 Size distribution by occurrence, liquid pressure 5 barg

Figure 5-5 shows the highest occurring sizes is between 100-119 µm for all three positions. Figure 5-5 also shows that the distribution pattern follows approximately the same trend for each position from the center. The span of the droplets in this test are from approximately 15 to 315 µm.

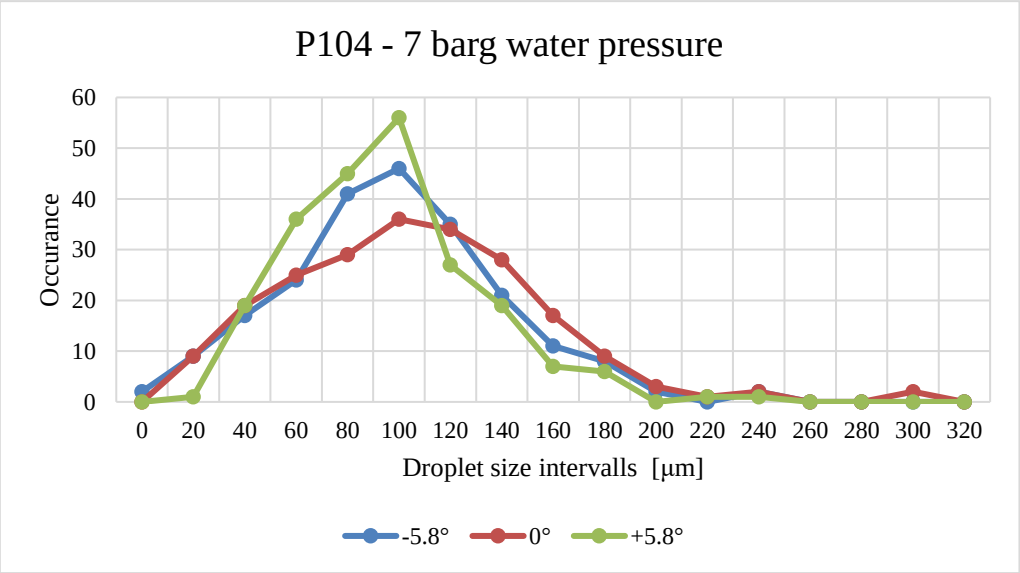

Figure 5-5 Size distribution by occurrence, liquid pressure 7 barg

Figure 5-6 shows highest occurring sizes is 50-99 µm for the center of spray and -5.8° from the center. +5.8° from the center has 100-149 µm as highest occurring size. Figure 5-6 also shows that the distribution pattern follows approximately the same trend for each position from the center, with the exception that +5.8° from the center the droplet sizes peak is in a larger interval. The span of the droplets in this test are from approximately 25 to 700 µm with 50-149 µm as the highest occurring size.

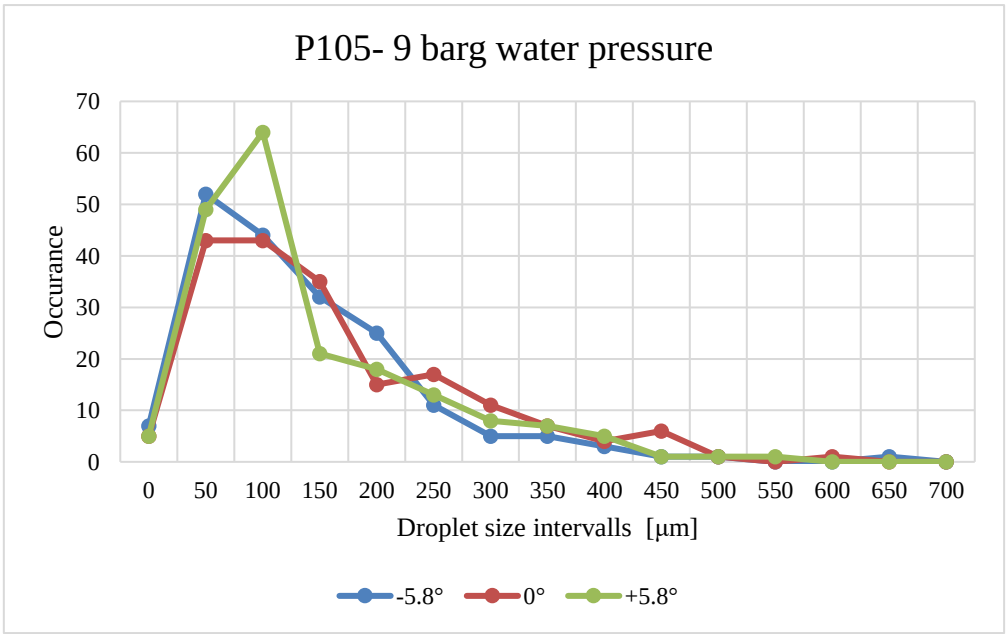

Figure 5-6 Size distribution by occurrence, liquid pressure 7 barg

Figure 5-2, 3, 4, 5 and 6 all show a low occurrence of large droplet sizes although the sizes increase with pressure increase. The figures also show that the distribution pattern follows approximately the same trend for each position from the center in all pressure tests, with some exceptions. The sizes measured +5.8° from the center of the spray shows tendencies to be larger than in center and -5.8° from the center of spray.
The total span of the droplets ranges from approximately 10 μm to 700 μm and the size of the span increases with pressure increase. The most occurrent size interval was approximately 70-99 μm.

5.2 Mass flow measurements

Figure 5-7 shows the measured mass flows for air and water. The values are the average of all measured flows for each test. The mass flow of air is almost constant, but decreases in pressure test 5 barg and increases, to some extent, in pressure tests 7 and 9 barg. The mass flow of water increases with the increase in pressure and it has the highest increase from 3 to 9 barg.

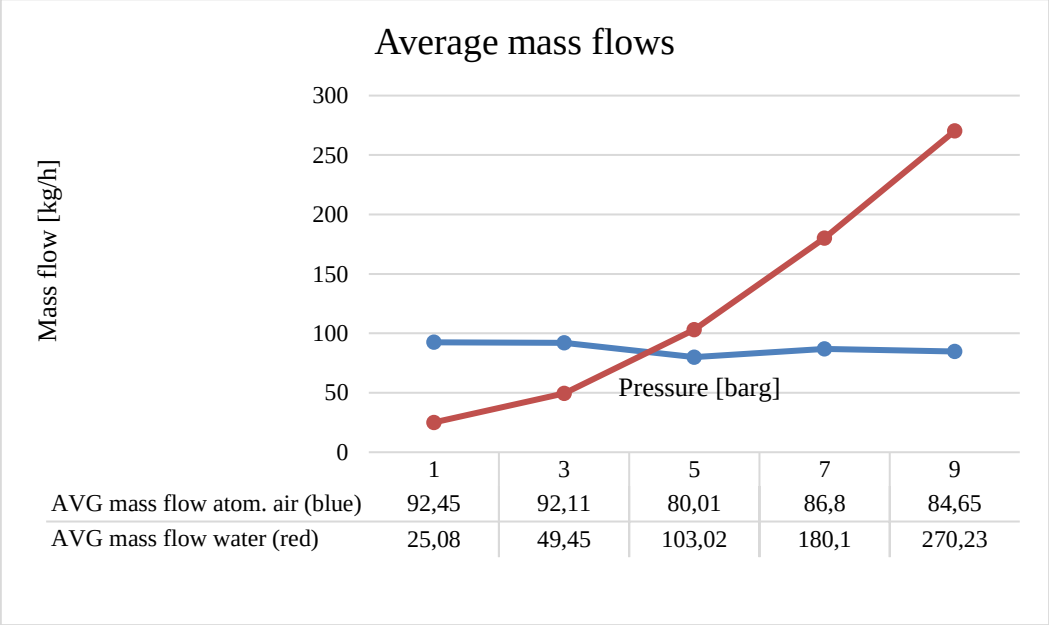

Pressure [barg]	1	3	5	7	9
AVG mass flow atom. air (blue)	92,45	92,11	80,01	86,8	84,65
AVG mass flow water (red)	25,08	49,45	103,02	180,1	270,23

Figure 5-7 Average mass flows for water and air

The turndown ratio, based on the mass flows of water, is 10.77 according to Table 5-2. The ratio is exceeding the ratio of the nozzle which is 1:10 with 0.77.

Table 5-2 Experimental turndown ratio

Experimentally measured mass flows of water $[\frac{kg}{h}]$		**Turndown ratio** $(\frac{Max}{Min})$
Max	**Min**	
270.23	25.08	10.77

5.3 Visual observations

This chapter shows raw video (frames) from the recording of the droplets. The test not present in this chapter consisted mostly of spherical droplets, assumed in its steady state. In other words, the tests not present in this chapter showed none, or no significant bulges or unbroken droplets or sheets of water.

Figure 5-8 shows the development of a droplet about to break up and to the point where it is broken up into two droplets with a string of water that used to bind them together. Non-spherical droplets are visible in the pictures, in the frame to the left, as well as in the picture to the right.

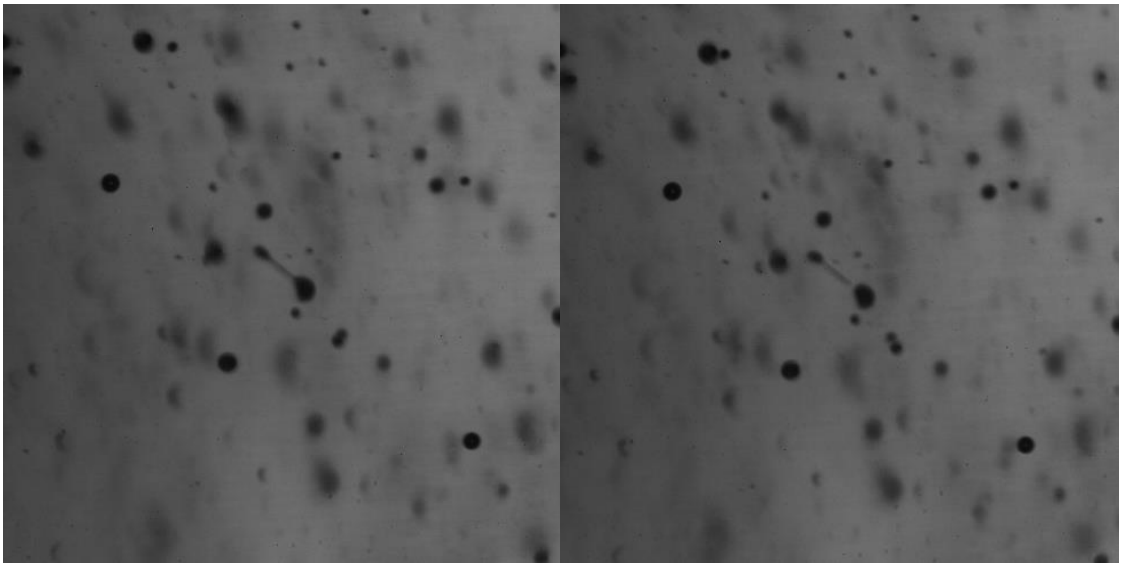

Figure 5-8 Water pressure 7 barg, in center of spray (0°)

Figure 5-9 shows sheets of water and bulges of droplets. Non-spherical droplets are visible in the pictures, in the frame to the left, as well as in the picture to the right.

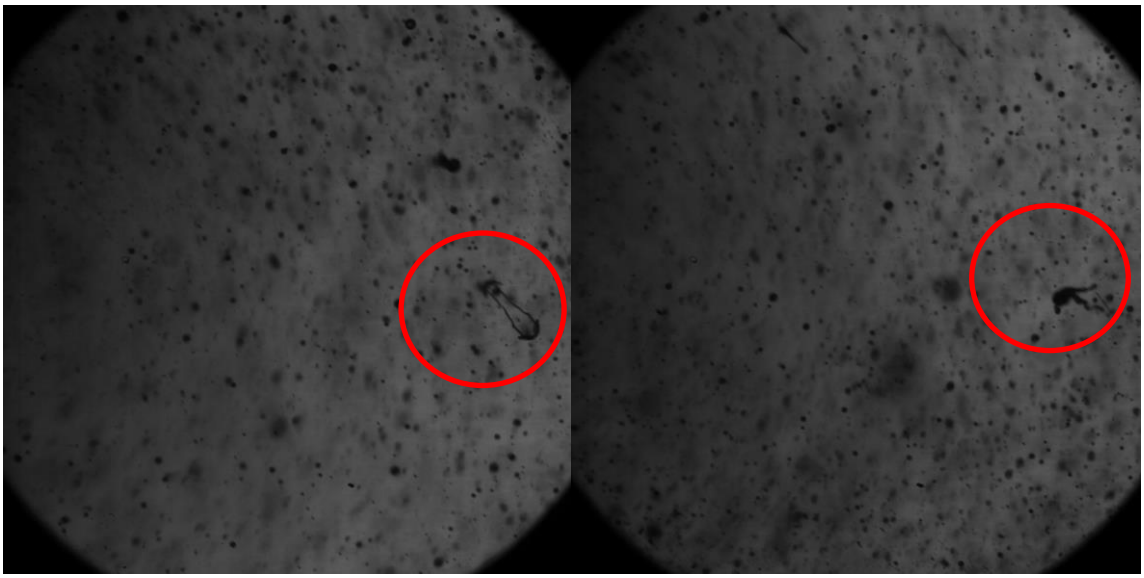

Figure 5-9 Water pressure 7 barg, +5.8° from the spray center

Figure 5-10 shows that bulges are visible in the picture to the left. A string of water is connecting two droplets together in the picture to the right. Non-spherical droplets are visible in the pictures, in the frame to the left, as well as in the picture to the right.

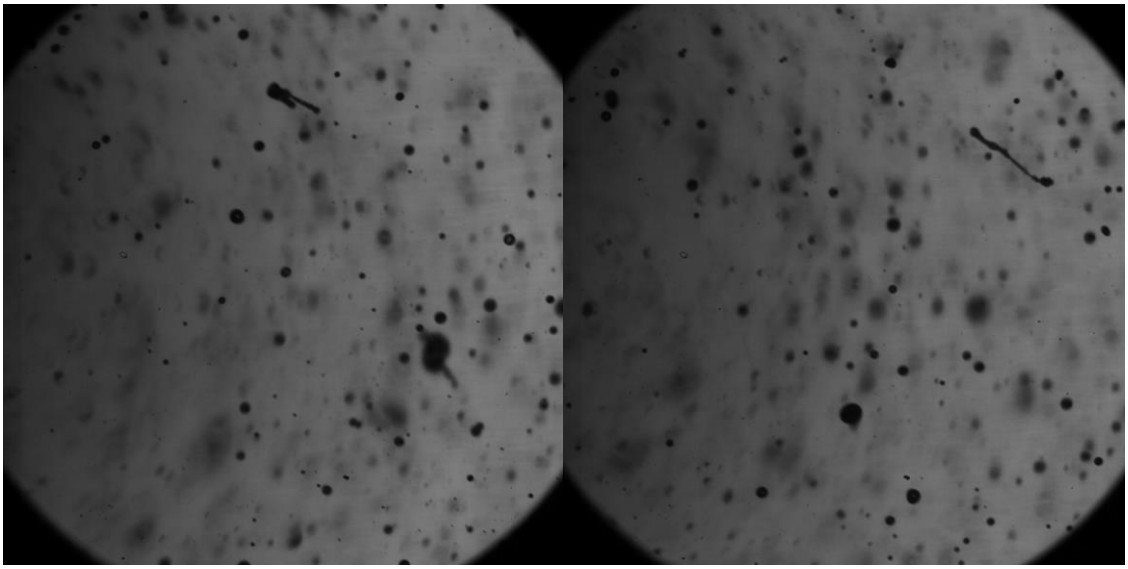

Figure 5-10 Water pressure 9 barg in center of spray (0°)

Figure 5-11 shows bulges present in the pictures. The picture to the left shows a bulge with a sheet of water. The bulges shapes are much larger than the surrounding droplets. Non-spherical droplets are visible in the pictures, in the frame to the left, as well as in the picture to the right.

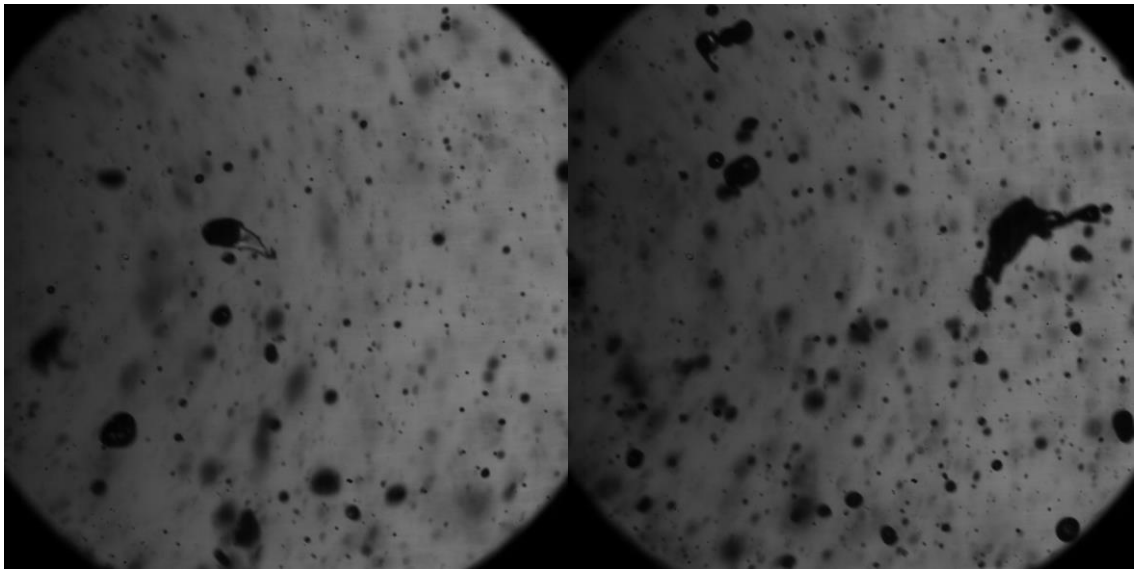

Figure 5-11 Water pressure 9 barg, +5.8° from the spray center

The results presented in this chapter contained bulges and droplets colliding or breaking apart. The identification of the droplets according to Hinze was mostly bulges. Non-spherical droplets are visible in all frames presented in this chapter.

6 Discussion

The tollgate method for sampling droplets brings the advantage of measuring non-spherical droplets; however, the equipment was not available in the facility, and the spatial method was sufficient to achieve results for droplet diameter analysis in this experiment. Pfeifer et al. used both spatial and temporal method for investigation of non-spherical droplets, which is a suitable suggestion for further analysis of the data collected in this thesis.

The measuring technique in MATLAB requires manual measurement of droplets via the operator (computer mouse), which is not necessary equally accurate for each measurement, possibly producing non-measurable deviation factors in the droplet measurements.
The code in MATLAB was initially producing duplicates of values, and not zeroes in the matrix when skipping frames, or there were no droplets available for measurement. The extra values made the resulting diameter measurements difficult to read. However, the duplicated/extra values were successfully removed, and the code was edited, showing only the measured values.

The width of one frame was measured to be approximately 0.832 cm and could have been used as a reference size for determining the position of the measurement points in the spray; it would have given a precise coverage of the spray width. If the experiment is to be repeated in the future, the frame size could be a good reference size when determining the positions to analyze.

The intended method for image processing was discharged due to change of equipment and lack of time, which was a result of the experimental delay this semester. The use of a similar imaging processing technique as Lundberg developed is highly recommended for further analysis. The droplets velocities and the flux are of great interest to determine for further characterization of the spray.

The main limitation of the shadowgraph technique used in this thesis was when creating a shadow to outline the droplets, the droplet is not the direct object of interest, instead the shadow is, which could have been misinterpreted in the image processing of the droplets.

Settings regarding the depth of field were challenging due to the limitation of the light source (IR laser), resulting in a slightly blurry depth of field. When calibrating the pixel size, the measurements were difficult to perform accurately, due to the blurry pixels when zooming, possibly resulting in a less accurate pixel size.

The test for the highest pressure was conducted twice due to uncertainties in the parameters, the second video was similar to the first, meaning the uncertainties was dismissed.
In the experimental procedure, there were many sources of error that could be a contributor to faulty data, such as the possibility of the spray not being fully atomized. Video footage, where it is presumed that the spray is fully atomized, could have been misinterpreted.
The position of the burner lance was changed during the experiment which resulted in misplacement of the nozzles perpendicularity to the camera and laser. This misplacement was corrected for each test and possibly resulted in a misplacement of the spray from the depth of field.

Movement from walking inside the rig could disturb the video by misplacing the spray. Another result of moving inside the container could be a disturbance of other equipment such as the laser position.
Settings in Photron FASTCAM Viewer for the high-speed camera was faulty the first six videos, the exposure settings were positive, not negative, deviating from Appendix D Experimental procedure. However, no faults or errors were registered in the videos.

Replacing diesel fuel with water is a recommended measure for non-combusting and low-pressure experiments for determination of the spray characteristics. However, little research (only Sulaiman et al.) was found to confirm a coherence between water and diesel spray. Further research is recommended to be able to confirm the coherence between the water and diesel.

According to the calculated SMD values the largest droplets occur in the center of the spray. However, according to the measured droplets in chapter 5.1.2 the distribution shows tendencies to be larger +5.8° from center. It is not possible to determine if the SMD values in this experiment will provide a sufficient combustion based on the volume to surface ratio of the spray distribution alone. Mainly due to a low number of measured droplets, but also according to Lefebvre. The SMD increased rapidly with increase in pressure, which can be a contributing factor to an unstable flame profile.

Occurrence results state that the largest droplets are found at the two highest pressure tests, as well as the bulges and large non-spherical droplets. Bulges and non-spherical droplets were not included in the measurements due to the limitation of the user defined measuring method in MATLAB. The largest droplet from the results is therefore limited to the largest spherical droplet from the measurement method, although larger droplets are presented in the results.
In chapter 5.1.2, it is commented; “The sizes measured +5.8° from the spray center shows tendencies to be larger than in center and to -5.8° from the center,” which can be true. However, due to the low amounts of measured droplets, it is not adequate to conclude that the droplets are, in fact, larger +5.8° from the spray center. The interval where most of the measured droplets sizes were found was approximately 50-149 µm.

The experiment exceeded the nozzles turndown ratio of 1:10. Due to water being heavier than diesel and has a higher surface tension than diesel, the mass flows for water needs to be greater. The maximum mass flow of water should have been 225 kg/h according to the turndown ratio of the nozzle, which would have given a maximum of 8 barg fuel pressure when testing. The exceeding of the turndown ratio is presumed to be the main contributor to poor atomization in the highest pressure test. However, the nozzles performance in the 7 barg test is not as good as the previous lower pressure tests which can be an implication to a lower quality of the nozzle at elevated pressures.
If the schematics for the atomizing pressure curves are to be followed, the highest recommended pressure of the diesel spray will be approximately 6.3 barg (with an air pressure at 6 barg).

In Figure 5-8 two droplets are separating, which can be a result of droplet collisions or a result of secondary atomization. In Figure 5-9 it is shown sheets of water, but the frame is very dark due to, what is most likely, water mist causing noise in the video. However, the bulges and sheets of water are still very visible.
Figure 5-10 shows the same droplet behavior as Figure 5-8 with possibly the same cause. However, the droplets in general are larger than in Figure 5-8.
Figure 5-11 is presenting similarities to Figure 5-9 and as the pressure increase indicate, the droplets in Figure 5-11 are larger as well.

The identification of the shapes of droplet disintegration from Hinze and Lefebvre is useful tools to determine the droplet shapes based on the surrounding aerodynamic flow patterns. From the results of this experiment, no lenticular or cigar shaped droplets were found.
Essentially, the results consisted of spherical droplets. However, findings of bulges and non-spherical droplets were significant. The shapes origin can be explained by more than just irregular surrounding flow, such as further breakup process, poor atomization and collisions between droplets.
The non-spherical droplets shape can be explained by drag from the surrounding aerodynamics, since the droplet is traveling with a high velocity compared to ambient surrounding air.
The colliding or not broken up droplets are quite visible in the frames, due to lack of tracking tools (like the tollgate method or Lundberg's program), it is impossible to determine if the droplets are about to break up further or about to stabilize without further break up (steady state).

Particles of unknow origin or other debris from the buffer pool could have entered the system when filming, which could result in misinterpretation of what is expected to be droplet shadows in the videos.

With regards to the droplet diameter span in this thesis, three separate sprays with a large variety of droplet sizes could create an unstable flame profile, e.g. a "dancing flame". A monodispersed spray is difficult to produce; however, investigation of other nozzles with a more consistent droplet distribution is recommended, to ensure a more stable flame profile and furthermore, a more stable combustion process if not other adequate adjustments are available.

Indications of the nozzles performance can be implied from this report based on the observation of the results of this experiment. The performance of the nozzle is adequate with the assumption that the droplet sizes are within acceptable limits for the users. The nozzle is performing adequately within the turndown ratio, with some exceptions in testing at 7 barg. The nozzle is producing a polydisperse spray with a wide span of droplet sizes.

7 Conclusion

The span of the droplet diameters was measured to be approximately from 10 µm to 700 µm regarding all the test result as a whole. The span of the droplet sizes increased with pressure increase. The highest occurring size was found between approximately 50-149 µm.

The nozzle produced bulges at elevated pressures, and the atomization was poor, therefore, exceeding the turndown ratio for the nozzle is not recommended, whether its water or diesel oil. The performance of the nozzle can be described as adequate within its limitations, with the anticipation that the diameter span is acceptable for the users of the atomizer.

A large diameter span in a polydisperse spray is not recommended as it can result in an unstable flame profile.

Replacing diesel fuel with water is a recommended measure for non-combusting and low-pressure experiments.

The SMD calculation for heat and mass transfer applications is an adequate addition to determining the spray characteristics, however not descriptive enough alone.

The user defined method for measuring droplet sizes in MATLAB was sufficient for analyzing the results in this thesis.

7.1 Suggestions for further research

The result presented in this thesis should be considered as an implication or accommodation for further work regarding atomization of spray. If further research is desirable, the collected data is available via Associate Professor, Joachim Lundberg, at University College of Southeast Norway.

The results and collected data from this report can contribute to a determination of the need to change the atomizing nozzle, for further optimization of the IGG system.

The data collected gives also opportunities for further analysis of the spray. One suggestion is to create a MATLAB script, e.g. a method similar to Joachim Lundberg's program for image processing. The second suggestion is a comparison study of spray characteristics of water compared to diesel spray.

A third suggestion is to use both spatial and temporal analysis if the experiment is to be reproduced. The final suggestion of this report is to use the frame size as a reference for measuring points to sufficiently cover the spray width.

References

[1] A. Hegab, A. La Rocca, and P. Shayler, "Towards keeping diesel fuel supply and demand in balance: Dual-fuelling of diesel engines with natural gas," *Renewable and Sustainable Energy Reviews*, vol. 70, pp. 666-697, 4// 2017.

[2] WÄRTSILÄ®. (2013). *MOSS INERT GAS GENERATOR SYSTEM FOR GAS CARRIERS*. Available: http://cdn.wartsila.com/docs/default-source/product-files/inert-gas/wartsila-moss-generator-system-for-cas-carriers.pdf?sfvrsn=4

[3] J. Xu, D. Testa, and P. K. Mukherjee, "The Use of LNG as a Marine Fuel: The International Regulatory Framework," *Ocean Development & International Law*, vol. 46, pp. 225-240, 2015.

[4] S. Lee, S. Seo, and D. Chang, "Fire risk comparison of fuel gas supply systems for LNG fuelled ships," *Journal of Natural Gas Science and Engineering*, vol. 27, Part 3, pp. 1788-1795, 11// 2015.

[5] O. I. Lindløv, "Text for charter_2017_04," Wärtsilä Ship Power / Environmental Solutions / Inert Gas / Technical and R&D2017.

[6] "Annual Energy Outlook 2017 with projections to 2050," ed. www.eia.gov/aeo: U.S Energy Information Administration, 2017.

[7] F. Burel, R. Taccani, and N. Zuliani, "Improving sustainability of maritime transport through utilization of Liquefied Natural Gas (LNG) for propulsion," *Energy*, vol. 57, pp. 412-420, 8/1/ 2013.

[8] M. Anderson, K. Salo, and E. Fridell, "Particle- and Gaseous Emissions from an LNG Powered Ship," *Environmental science & technology*, vol. 49, p. 12568, 2015.

[9] O. I. Lindløv, "IGS R&D IGS010 (part 2)," Wärtsilä Ship Power / Environmental Solutions / Inert Gas / Technical and R&D2016.

[10] Y. Shi, "Reducing greenhouse gas emissions from international shipping: Is it time to consider market-based measures?," *Marine Policy*, vol. 64, pp. 123-134, 2// 2016.

[11] J. Lundberg, T. Høgskolen i, and e. o. m. Høgskolen i Telemark Institutt for prosess, "Image-based sizing techniques for fire water droplets," 5:2015, Telemark University College, Faculty of Technology, Department of Process-, Energy and Environmental Technology, Porsgrunn, 2015.

[12] A. H. Lefebvre, *Atomization and sprays*. Boca Raton, FL: CRC press, 1989.

[13] J. Hinze, "Fundamentals of the hydrodynamic mechanism of splitting in dispersion processes," *AIChE Journal*, vol. 1, pp. 289-295, 1955.

[14] S. Y. Lee and Y. D. Kim, "Sizing of spray particles using image processing technique," *Journal of Mechanical Science and Technology*, vol. 18, pp. 879-894, 2004.

[15] G. S. Settles, *Schlieren and shadowgraph techniques : visualizing phenomena in transparent media*. Berlin: Springer, 2001.

[16] G. L. Borman and K. W. Ragland, *Combustion engineering*. Boston: WCB McGraw-Hill, 1998.

[17] C. Pfeifer, D. Kuhn, and A. G. Class, "Coupled measurement of droplet size distribution and velocity distribution in a fuel spray with digital imaging analysis under elevated pressure," in *15th International symposium on applications of laser techniques to fluid mechanics. Lisboa, Portugal:[sn]*, 2010.

[18] R. A. Mugele and H. D. Evans, "Droplet Size Distribution in Sprays," *Industrial & Engineering Chemistry*, vol. 43, pp. 1317-1324, 1951.

[19] S. A. Sulaiman and M. H. Daud, "Comparative Study of Droplet Sizes of Water and Diesel Sprays," *Asian Journal of Scientific Research*, vol. 6, p. 367, 2013.

[20] O. I. Lindløv, "NOZZLE SPRAY ANGLE AND SPRAY DISTRIBUTION " WÄRTSILÄ Moss AS 2016.

[21] O. I. Lindløv, "PROJECT NAME: PILOT BURNER

" WÄRTSILÄ Moss AS 2016.

[22] LaVision, "Long Distance Microscopes," ed, 2015.

Appendices

Appendix A Task Description

University College of Southeast Norway

www.usn.no

FMH606 Master's Thesis

Title: Experimental measurements of diesel spay in an inert gas generator

TUC supervisor: Joachim Lundberg

External partner: Wärtsilä Moss AS (Odd Ivar Lindløv)

Task background:

Wärtsilä Moss AS develop, design, sell and execute projects related to inert gas generation. The inert gas is either CO_2 (from combustion of liquid of gaseous fuels), with a low oxygen content (0.5 to 3 vol%), or nitrogen produced by membrane separation of air (typical oxygen content 0.5 to 5 vol%). These systems are used in transportation of hydrocarbon fuels to ensure an inert atmosphere where the fuel is stored.
The inert gas generator burner (all types burning diesel oil) is designed around a nozzle that uses pressure for atomizing (i.e. mechanical atomization). The smaller capacity systems use a nozzle with 1:4 turndown[1] capability, whereas the larger ones (in particular inert gas systems for LNG carriers systems) use a nozzle with no turndown at all. Earlier tests (visual verification) as well as operational data point towards a too poor atomizing when using this particular nozzle for turndown, resulting in combustion issues (high CO, less stable O_2). The main drawbacks with mechanical atomization is a poor turndown capability and the fact that a higher pressure is required to achieve atomization.
The alternative atomizing method is to use air as atomizing medium (for heavier oils (residuals), steam is commonly used, but the diesel oil used is of good refined quality). The benefit is that this requires lower diesel oil pressure (and an alternative pump technology can be used) as well as makes it possible to achieve a far better turndown ratio (up to 1:10). The drawback is that air is required at a certain flow rate and pressure during burner operation.

The droplet size distribution is expected to be very important for the combustion of the diesel spray. Larger droplets will give more CO and small droplets are hard to generate. The existing equipment for generating droplets does not have a well-documented size distribution and it is expected that the distribution will change with turndown ratio.

Task description:

The target of the task is to measure the droplet size and spray distribution of a new nozzle when operating with a large turndown ratio (1:10). In this test the diesel will be

[1] Turndown refers to the operational range of a device. e.g. a nozzle with a maximum flow of 10 that can be used at flows of 1, has a turndown ratio of 1:10, ref Wikipedia.

replaced with water for environmental reasons. For the test, the measurement will be conducted in line with Mr Joachim Lundberg's (HSN) PhD thesis '*Image-based sizing techniques for fire water droplets*' (ISBN 978-82-7206-402-9). This is an image-based measurement system developed at HSN. The test rig setup will be based around the principle as shown in figure 3.3 (page 29) in the mentioned thesis. A literature review will be conducted to achieve a sufficient level of knowledge on the topic.

Student Category:

PT or EET; experience from experimental research is an advantage, but not a requirement.

Practical arrangements:

The measurement rig will be located at HSN. The inert gas generator will be provided by Wärtsilä, and the measurement equipment is already available at HSN.

Signatures:

Student (date and signature):

30/1-17

Supervisor (date and signature):

30/1 - 2017

Appendix B MATLAB Script

```
clear all
clc

f='C:\Users\Lena Dyveke\Documents\MATLAB\170404LeW_P105_T007_C001H001S0001'; %Filename
files = dir([f '\*.tif']);
num_files =numel(files);

npp=8; %micrometres per pixel

%max number of droplets
md=3;

%Help sizes
t = 0:0.1:2*pi;
D=zeros(1,md);
diam=D;
%Read images
for k=600:10:1000 % k is optional within 1 to 2048. The code skips 10 frames due to low
velocity
I = imread([f '\',files(k).name]);
D=zeros(1,md);
imshow(I)
next=0;
i=1;
while next==0

   hold on
   rectangle('Position',[40,35,100,30],'FaceColor','White')
    text(50,50,num2str(i));

[x1, y1]=ginput(1);
if or(and(and(and(x1<140,y1>35),x1>40),y1<65),i>md)
    next=1;
else

plot(x1,y1,'+')
[x2, y2]=ginput(1);
plot(x2,y2,'+')
center=[x1-(x1-x2)./2 y1-(y1-y2)./2];
r=sqrt(((x1-x2)./2)^2+((y1-y2)./2)^2);
x = r*cos(t);
y = r*sin(t);
plot(x+center(1),y+center(2),'Color','r')

d(i)=2*r;
D(i)=d(i)*npp
hold off
end

i=i+1;
end
diam=[diam;D];
end
```

Appendix C Safe Job Analysis (SJA)

EXECUTED BY: Lena Dyveke Weber				
AREA: A-103 Machine hall, Droplet rig				
DATE: 04.04.2017-04.04.2017			**HSE - MSDS: YES ☐ NO X**	
PARTICIPANTS:	**DEPARTMENT**	**SIGNATURE**		
Lena Dyveke Weber	**PEM-student**			
NO	**ACTIVITY DESCRIPTION**	**RISK DESCRIPTION**	**SAFETY MEASURES**	**RESPONSIBLE / DEADLINE**
1	**Using FIREFLY Laser Class 4**	**Eye exposure can cause damage**	**Use correct goggles, restrict area during experiment**	**L.D.W**
2	**Water spray**	**Damage to equipment**	**Waterproof/secure equipment**	
3	**Falling/stumble**	**Human injuries and/or damage to equipment**	**Use Adam Hall cable protector where the cables are in passage ways and place equipment properly. Wet surfaces must be dried/cleaned up**	**L.D.W**
4	**Using frequency controlled water pump**	**Fire/destroy pump**	**Do not leave the pump running to a closed valve**	**L.D.W**
5	**Data documentation**	**Faulty data/results**	**Document experiments in detail to make sure it is reproducible**	**L.D.W**
6	**Ventilation**	**Destroy expensive equipment**	**Always start the moisture removing system after the rig is used and open door and window to prevent residue water/mist from entering the high-speed camera and laser cases**	**L.D.W**
7	**Loose hoses under pressure**	**Human injuries and/or damage to equipment**	**Installation must be performed correctly**	**L.D.W**
8	**Rapid/rash movement in caravan**	**Movement of camera and burner lance position could result in faulty data/results**	**Move quietly and swiftly**	**L.D.W**

Appendix D Experimental procedure

Procedure for high-speed camera and FIREFLY laser, for measuring water droplets (diesel)

Testing of nozzle 24-Y-90°-00-3 with reverse disc 24-R with water pressure 1, 3, 5, 7 and 9 barg pressure. The atomizing air pressure is to be constant at 6 barg, see Figure 0-1. The position of the burner lance is to be tested in 9 positions. The positions are determined with extrapolation with trigonometry and are presented in Figure 0-2.

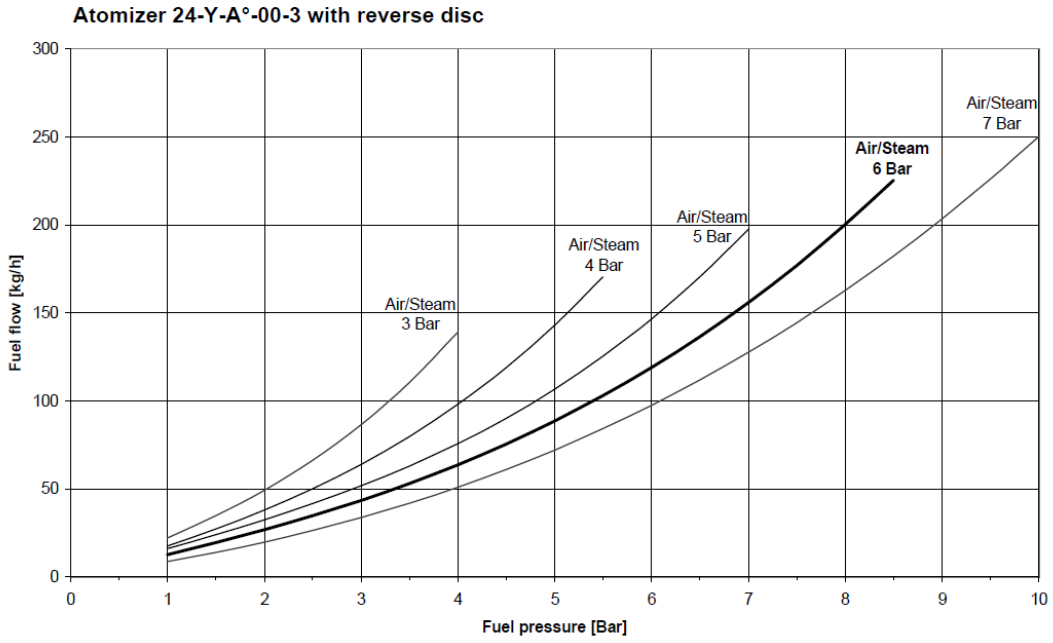

Figure 0-1 Pressure curves and mass flows for liquid fuel and atomizing air/steam. Start/Initial is at fuel pressure 1 barg

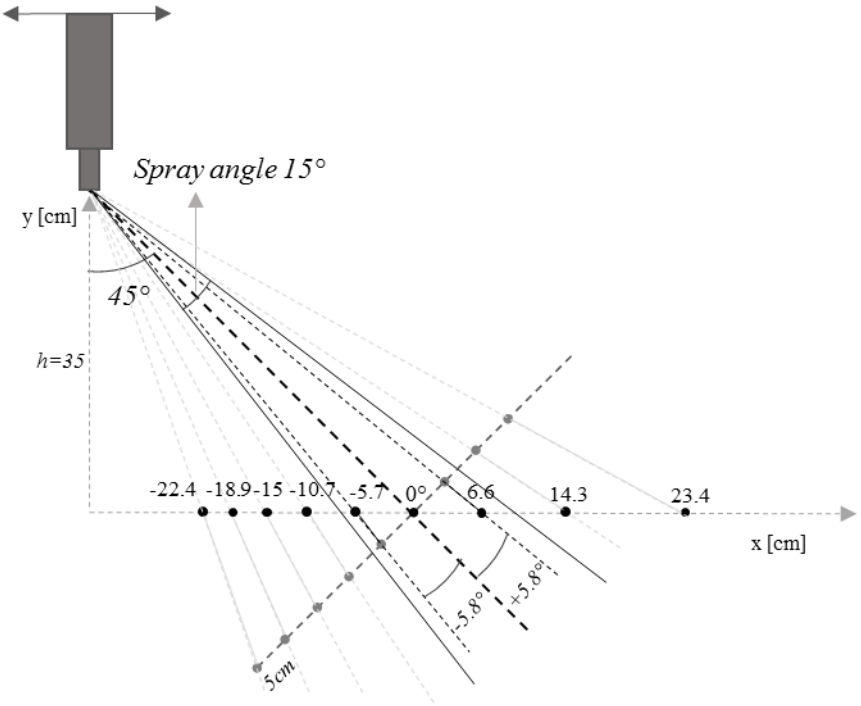

Figure 0-2 Measuring points in x-axis for burner lance with reverse disc and nozzle 90°

Preparations for experiment

- Connect camera to a laptop with Photron (make sure power is available for laptop)
- Safety procedures must be in motion before the laser ignites- lock area and light warning lamps. Use prepared SJA form for confirming safety precautions
- Set correct settings in FIREFLY laser
    - Duration 3 µs
    - Separation 10 µs
    - Delay 328 µs
    - Number of pulses 2
    - Connection ext/2-ve, connect in position IP from camera
- Set camera exposure to negative in camera settings in Photron and the frame rate to 3000 frames per second
- Initiate laser lamp (use goggles) and press Shading in Live in Photron, need to repeat this step only if camera has been powered off
- Calibrate the camera depth of field with a Patterson globe, no need to repeat this step once performed. Make sure not to move any of the equipment causing the depth of field to shift.
    - Take a snapshot with Photron in depth of field and move the translation screw 1mm away from the depth of field. Move the translation screw 10 mm away and toward the camera, remember to take a snapshot of every step (20 snapshots in total). The snapshot in the depth of field is for calibration of pixel size for further analysis in MATLAB

Experiment

The position of the burner lance will be regulated with each sequence to make sure sufficient data is collected, look to Figure 0-1 for positions.

- Regulate position of nozzle
- Initiate fluid flow (via frequency controlled pump)
- Initiate air pressure (6 barg) from regulator located at wall
- Read pressure gauges for air and fluid mounted on burner lance- regulate rpm via frequency controller. Air can be regulated located at the wall (no need to regulate once set to 6 barg)
- Take photography recording with the camera and download movie to an external hard drive
    - Name the video 17xxxxLeW_P10x_T00x and save as .tif
- Read off the values for mass flows (Coriolis)
- Shut down or pauses between videos:
    - Stop air flow
    - Stop fluid flow
    - Plug out power for frequency controlled pump and/or other devices for longer pauses
- Aerate in between sequences to remove water mist

After experiment

- Camera equipment must be dismantled, and placed in proper carriers. If the experiment is to be continued, do as follows:
    - Close camera lenses with covers
    - Start the moisture remover device and secure it
- The nozzle must be demounted and blow dried and stored dry. If experiment is continued let the nozzle be
- Empty the buffer pool, open valve located at the bottom of the pool

Appendix E Nozzle with reverse disc

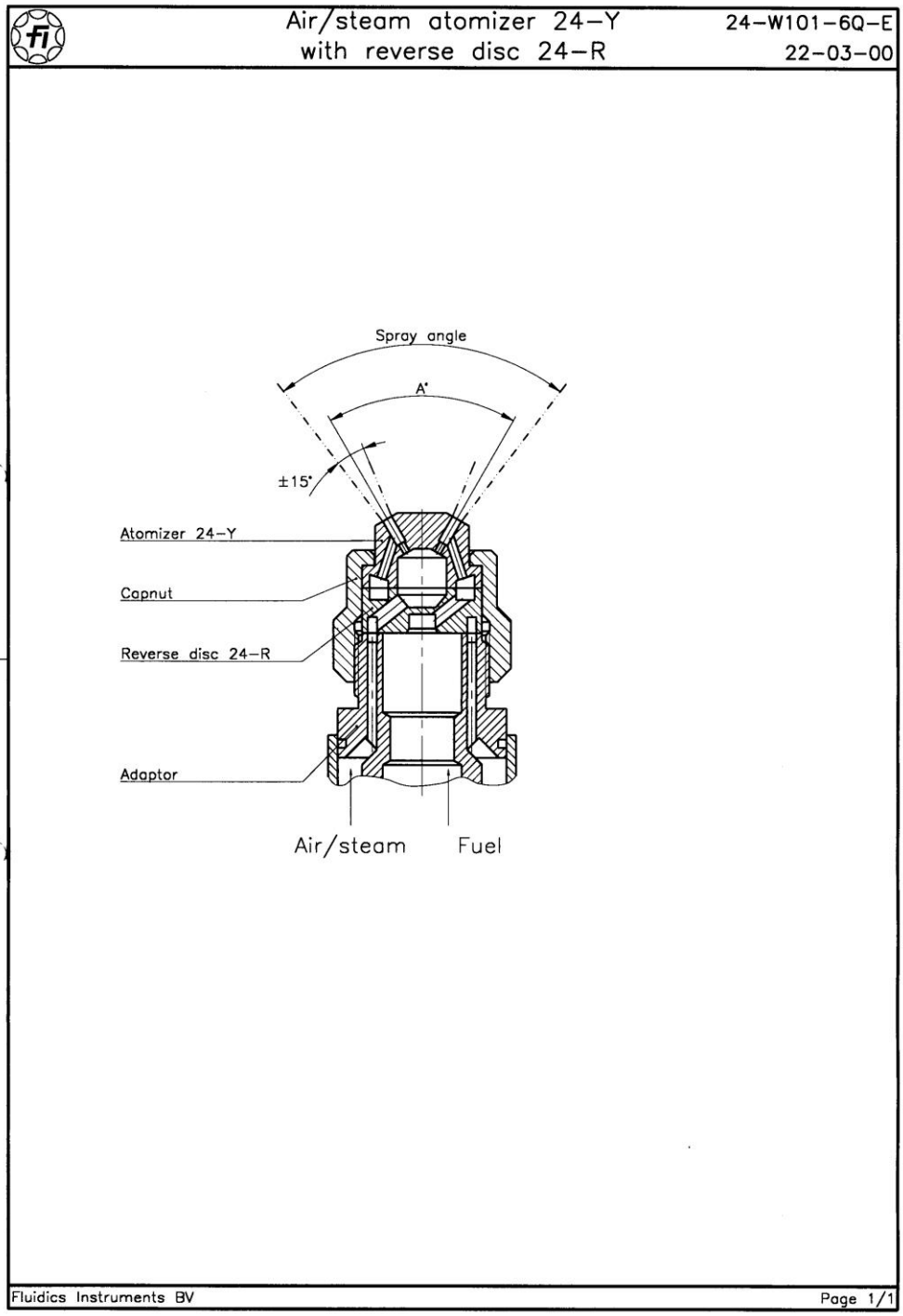

Figure 0-3 Air/steam atomizer 24-Y with reverse disc 24-R

Appendix F Nozzle 24-Y

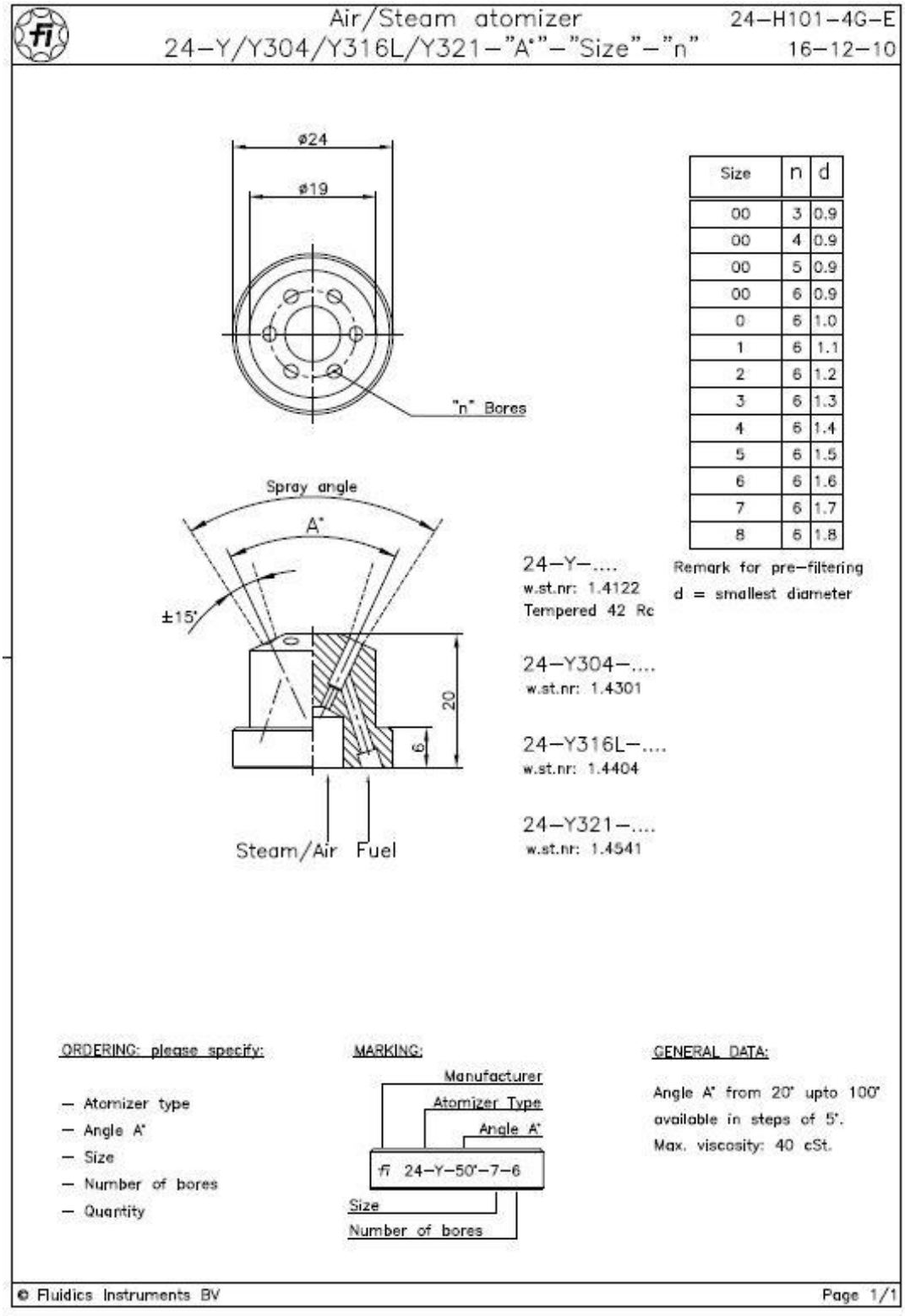

Figure 0-4 Air/Steam atomizer 24-Y

Appendix G Burner lance 24

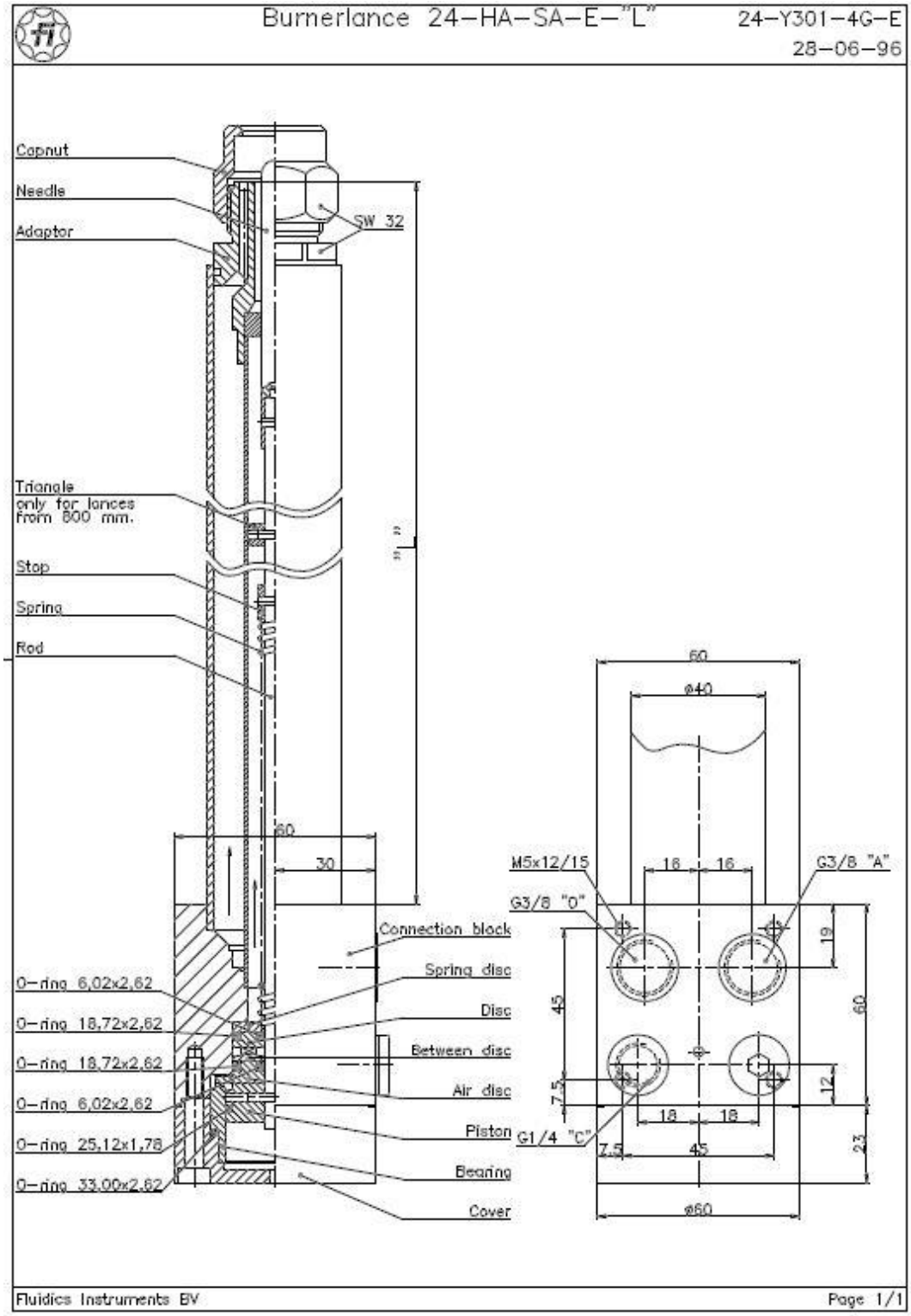

Figure 0-5 Burner lance 24-HA-SA-E-«L»

Appendix H Gear Pump

WÄRTSILÄ

General document

Title:	ATTACHMENT 2	**Doc.ID:**	
		Revision:	
Author:		**Status:**	Draft
Draft by:	/	**Pages:**	1 (1)
Organisation:			
Project number and name:	/		

attachment 2.docx

1" Selvsugende Tannhjulspumpe
Type: WLZ008
Medium: Vann
Viskositet: 1 cp
Medium temperatur: 20 °C
Omgivelses temperatur: antatt 25 °C
Kapasitet: 10-300 l/h
Trykk: 8 bar
Materiale pumpehus og deksel: Messing OT58
Materiale akslinger: AISI316L
Materiale tannhjul: AISI316L / Plastmateriale KK
Mekanisk akseltetning: Ceramic/Graphite/FPM
Anslutninger: 3/8" BSP - Horisontale
Komplett pumpe med motor i lanterneutførelse
Motor: 0,75 kW – 230/440V – 50Hz – IP55 – B3/B14 – 1450 rpm – PTC
Maling: RED RAL 3003

Figure 0-6 Gear pump

Appendix I Frequency Controller

WÄRTSILÄ

General document

Title:	ATTACHMENT 3	**Doc.ID:**	
		Revision:	
Author:		**Status:**	Draft
Draft by:	/	**Pages:**	1 (1)
Organisation:			
Project number and name:	/		

attachment 3.docx

Frekvensomformer
Type: MC07B0008-2B1-4-00
Byggestørrelse: 0S
Enhetsutførelse: Standard Versjon
Integrert linjefilter: Kategori C1
Spenning: 1x200-240V
Strøm: 9,9 A
Frekvens: 50-60Hz (+/-5%)
Effekt: 0,75 kW
Nominell utgående effekt: 1,00 Hp
Utgangs merkestrøm: 4,2 A
Speed range: 0-5500 1/min
Omgivelsestemperatur min: -10 °C
Omgivelsestemperatur max: +50 °C
Beskyttelse: IP20
Parametreringstastatur: FBG11B – IP20

Figure 0-7 Frequency controller